Bacterial catabolic system of acetovanillone and acetosyringone useful for upgrading aromatic compounds obtained through chemical lignin depolymerization

Running title: Acetovanillone/acetosyringone carboxylase system

Yudai Higuchi[a,b], Naofumi Kamimura[a], Hiroki Takenami[a], Yusei Kikuiri[a], Chieko Yasuta[b], Kenta Tanatani[a], Toru Shobuda[a], Yuichiro Otsuka[c], Masaya Nakamura[c], Tomonori Sonoki[b], and Eiji Masai[a]

[a] Department of Materials Science and Bioengineering, Nagaoka University of Technology, Nagaoka, Niigata, Japan

[b]Faculty of Agriculture and Life Science, Hirosaki University, Hirosaki, Aomori, Japan

[c] Department of Forest Resource Chemistry, Forestry and Forest Products Research Institute, Tsukuba, Ibaraki, Japan

Address correspondence to Eiji Masai, emasai@vos.nagaokaut.ac.jp

Y.H. and N.K. contributed equally to this work. Author order was determined on the basis of their contributions to the writing of the manuscript.

ABSTRACT

Acetovanillone is a major aromatic monomer produced in oxidative/base-catalyzed lignin depolymerization. However, the production of chemical products from acetovanillone has not been explored due to the lack of information on the microbial acetovanillone catabolic system. Here *acvABCDEF* was identified as specifically induced genes during the growth of *Sphingobium* sp. strain SYK-6 cells with acetovanillone and these genes were essential for SYK-6 growth on acetovanillone and acetosyringone (a syringyl-type acetophenone derivative). AcvAB and AcvF produced in *Escherichia coli* phosphorylated acetovanillone/acetosyringone and dephosphorylated the phosphorylated acetovanillone/acetosyringone, respectively. AcvCDE produced in *Sphingobium japonicum* UT26S converted the dephosphorylated phosphorylated acetovanillone/acetosyringone intermediate into vanilloyl acetic acid/3-(4-hydroxy-3,5-dimethoxyphenyl)-3-oxopropanoic acid through carboxylation. To demonstrate the feasibility of producing *cis*,*cis*-muconic acid from acetovanillone, a metabolic modification on a mutant of *Pseudomonas* sp. strain NGC7 that accumulates *cis*,*cis*-muconic acid from catechol was performed. The resulting strain expressing *vceA* and *vceB* required for converting vanilloyl acetic acid to vanillic acid and *aroY* encoding protocatechuic acid decarboxylase in addition to *acvABCDEF* successfully converted 1.2 mM acetovanillone to approximate equimolar *cis*,*cis*-muconic acid. Our results are expected to help improve the yield and purity of value-added chemical production from lignin through biological funneling.

IMPORTANCE

In the alkaline oxidation of lignin, aromatic aldehydes (vanillin, syringaldehyde, and *p*-hydroxybenzaldehyde), aromatic acids (vanillic acid, syringic acid, and *p*-hydroxybenzoic acid), and acetophenone-related compounds (acetovanillone, acetosyringone, and 4'-hydroxyacetophenone) are produced as major aromatic monomers. Also, base-catalyzed depolymerization of guaiacyl lignin resulted in vanillin, vanillic acid, guaiacol, and acetovanillone as primary aromatic monomers. To date, microbial catabolic systems of vanillin, vanillic acid, and guaiacol have been well characterized, and the production of value-added chemicals from them has also been explored. However, due to the lack of information on the microbial acetovanillone and acetosyringone catabolic system, chemical production from acetovanillone and acetosyringone has not been achieved. This is the first study to elucidate the acetovanillone/acetosyringone catabolic system, and to demonstrate the potential of using these genes for value-added chemicals production from these compounds.

KEYWORDS

Sphingobium sp. SYK-6; lignin; acetophenone; biotin-dependent carboxylase; *cis*,*cis*-muconic acid

INTRODUCTION

The use of lignocellulosic biomass is expected to build a decarbonized society that breaks away from fossil resources. The development of lignin utilization has become particularly important in the utilization of lignocellulose. Lignin content in lignocellulose ranges from 9% to 32% (1), and gymnosperm (softwood) lignins are composed of guaiacyl (G) units with small amounts of *p*-hydroxyphenyl (H) units, whereas angiosperm (hardwood) lignins are composed of G-units and syringyl (S) units (2, 3). Grass lignins contain G- and S-units and more H-units than gymnosperm lignins (2, 3). Because of lingin's complex and heterogeneous structure, it is difficult to selectively extract specific compounds even when it is degraded, and it has been ineffectively used so far (1, 4). Recently, "biological funneling," in which a heterogeneous mixture of low-molecular-weight aromatic compounds obtained from chemo-catalytic depolymerization of lignin is converged to specific value-added chemicals, such as *cis*,*cis*-muconic acid (ccMA) and 2-pyrone-4,6-dicarboxylic acid using microbial catabolic functions, has attracted attention (5-12).

In the alkaline oxidation of lignin, aromatic aldehydes (vanillin, syringaldehyde, and *p*-hydroxybenzaldehyde), aromatic acids (vanillic acid, syringic acid, and *p*-hydroxybenzoic acid), and acetophenone-related compounds [acetovanillone (AV), acetosyringone (AS; a syringyl-type acetophenone derivative), and 4'-hydroxyacetophenone (a *p*-hydroxyphenyl-type acetophenone derivative)] are produced as major aromatic monomers (13-15). Base-catalyzed Indulin AT (a pine kraft lignin) depolymerization resulted in the formation of vanillin, vanillic acid, guaiacol, and AV as

84 major aromatic monomers, similar to the alkaline oxidation of Lignoboost lignin (a
85 softwood kraft technical lignin) (8, 16-19). A black liquor produced in a softwood kraft
86 pulping process, Lignoforce, contained guaiacol, vanillin, and AV as major aromatic
87 monomers (20). Among these major aromatic monomers, microbial catabolic systems of
88 vanillin, vanillic acid, and guaiacol have been characterized (21-29). Additionally,
89 value-added chemical production from vanillin, vanillic acid, and guaiacol has also been
90 explored (12, 18, 30-36). However, due to the lack of information on the microbial AV
91 catabolic system, chemical production from AV has not been reported (16, 18, 19).
92 Therefore, chemical production from all of the major aromatic monomers produced by
93 oxidative/base-catalyzed lignin depolymerization has been unachieved. Recently, Eltis
94 and coworkers isolated *Rhodococcus rhodochrous* GD01 and GD02, which can utilize
95 AV in addition to vanillin, vanillic acid, and guaiacol in the black liquor produced
96 during the Lignoforce kraft pulping of softwood (20). Based on the observation that
97 *apkC* was induced when GD02 was cultured in black liquor extracts containing AV,
98 *apkA-apkB-apkC*, presumed to encode biotin-dependent carboxylase, were predicted to
99 be involved in AV catabolism. However, the enzymatic system encoded by these genes
100 is unknown. Additionally, in *Arthrobacter* sp. strain TGJ4, 4'-hydroxyacetophenone and
101 AV are converted to 4-hydroxybenzoic acid and vanillic acid, respectively; however, the
102 enzymatic system has been unclarified (37).

103 *Sphingobium* sp. strain SYK-6 can utilize various lignin-derived dimers, such as β-
104 aryl ether, biphenyl, phenylcoumaran, and diarylpropane, as well as monomers,
105 including ferulic acid, vanillin, vanillic acid, and AV (11, 16, 20, 38, 39). In SYK-6

106 cells, stereoisomers of β-aryl ether model compound, guaiacylglycerol-β-guaiacyl ether,
107 are stereospecifically converted to achiral β-hydroxypropiovanillone (HPV) via Cα-
108 oxidation, ether cleavage, and glutathione removal (Fig. 1) (38, 40-44). HPV and β-
109 hydroxypropiosyringone (HPS, a syringyl-type β-aryl ether metabolite) are oxidized to
110 vanilloyl acetic acid (VAA) and 3-(4-hydroxy-3,5-dimethoxyphenyl)-3-oxopropanoic
111 acid (SAA), respectively, and further catabolized via vanillic acid and syringic acid.
112 (Fig. 1) (45). Additionally, we identified *vceA* and *vceB*, which encode an acetyl-CoA-
113 dependent VAA/SAA-converting enzyme and a vanilloyl-CoA/syringoyl-CoA
114 thioesterase, respectively (5). However, these enzyme genes were found to be not
115 essential for VAA/SAA catabolism in SYK-6. It has been reported that VAA is
116 chemically unstable and can be converted to AV by a non-enzymatic decarboxylation
117 (46, 47). Indeed, when an SYK-6 cell extract was incubated with HPV, a small amount
118 of AV along with VAA was generated (Fig. 1) (45).

119 In this study, the catabolic pathway of AV and AS in SYK-6 was determined, an
120 SYK-6 gene cluster consisting of six novel genes involved in AV and AS catabolism
121 was identified, and their functions clarified (Fig. 1). Furthermore, these genes were
122 expressed in a derivative strain of *Pseudomonas* sp. strain NGC7 (Shinoda et al., 2019),
123 which is expected to be a chassis microorganism for converting lignin-related
124 compounds, and this engineered strain successfully produced ccMA from AV.

RESULTS

Determination of the AV catabolism pathway in *Sphingobium* sp. SYK-6.

Intermediate metabolites generated during SYK-6 incubation with AV were identified to determine the catabolic pathway of AV in SYK-6. SYK-6 cells grown with AV were incubated with 1 mM AV in Wx minimal medium (48) for 33 h, and high-performance liquid chromatography (HPLC)–mass spectrometry (MS) analyzed the supernatant of the reaction mixture. This analysis indicated that AV disappeared and was converted into compounds I and II with retention times of 2.2 and 2.5 min, respectively (Fig. 2A and B). Based on the comparison of the retention time and the mass spectrum of compound I with those of the authentic sample, this compound was identified as vanillic acid (molecular weight [MW], 168) (Fig. 2C and E, Fig. S1). Furthermore, compound II was found to be VAA (MW, 210) by comparing with the retention time and the mass spectrum of the authentic sample (Fig. 2D and Fig. S1). These results suggest that AV was carboxylated, converted to VAA, and catabolized via vanillic acid in SYK-6 (Fig. 1).

Search for genes involved in the conversion of AV using microarray analysis.

The AV conversion rate was measured using SYK-6 cells grown in Wx-containing 10 mM sucrose, 10 mM glutamic acid, 0.13 mM methionine, and 10 mM proline (Wx-SEMP; the non-inducing condition) and Wx-SEMP containing 5 mM AV (the inducing condition) to investigate the inducibility of converting AV in SYK-6. The conversion rate of 1 mM AV by cells grown under the inducing condition was approximately 27-

147 times higher than that of cells grown under the non-inducing condition (Fig. S2). Thus,
148 the AV-converting enzyme gene(s) was induced by AV and/or its intermediates.
149 The AV-converting enzyme gene(s) was searched based on the induction profiles of
150 the entire SYK-6 genes analyzed by previous DNA microarray analysis (49). This
151 analysis indicated that six consecutive genes consisting of SLG_06540, SLG_06530,
152 SLG_06520, SLG_06510, SLG_06500, and SLG_06490 were induced 17–76-fold,
153 during SYK-6 growth with AV (Fig. 1B, Table S1). Among these genes, SLG_06540
154 and SLG_06530 showed 44% and 41% amino acid sequence identity, respectively, with
155 Proteins 1 and 2, which comprise phenylphosphate synthase involved in biotin and
156 thiamine diphosphate-independent phenol carboxylation by *Thauera aromatica* K172
157 (Table S2) (50-52). SLG_06520 and SLG_06510 showed 36% and 50% amino acid
158 sequence identity with a biotin carboxyl carrier protein (BCCP; AccB) and biotin
159 carboxylase (BC; AccC) of biotin-dependent acetyl-CoA carboxylase of *Bacillus*
160 *subtilis* 168, respectively (Table S2) (53). SLG_06500 showed 26% amino acid
161 sequence identity with the carboxytransferase (CT; PycB) of biotin-dependent pyruvic
162 acid carboxylase of *Methanothermobacter thermautotrophicus* ΔH (Table S2) (54).
163 These facts suggest that SLG_06520, SLG_06510, and SLG_06500 encode BCCP, BC,
164 and CT, of biotin-dependent carboxylase, respectively (Tong, 2013). The proteomic
165 analysis of the *Aromatoleum aromaticum* EbN1 grown with 4'-hydroxyacetophenone
166 revealed the upregulation of XccA and XccB, presumably biotin-dependent carboxylase
167 components, and *xccA-xccC-xccB* are predicted to be involved in 4'-
168 hydroxyacetophenone carboxylation (55). XccA (CT), XccC (BC), and XccB (BCCP)

169 have 55%, 63%, and 45% amino acid sequence identity with SLG_06500, SLG_06510,
170 and SLG_06520, respectively (Table S2). Furthermore, SLG_06500, SLG_06510, and
171 SLG_06520 exhibited 42%, 51%, and 38% amino acid sequence identity, respectively,
172 with *apkA* (CT), *apkB* (BC), and *apkC* (BCCP), the recently predicted AV catabolic
173 enzyme genes in *R. rhodochrous* GD02 (Table S2) (20). SLG_06490 showed 23%
174 amino acid sequence identity with NagD, a ribonucleotide monophosphatase of *E. coli*
175 K-12, belonging to the haloacid dehydrogenase (HAD) superfamily (Table S2) (56).
176 In *T. aromatica* K172, phenol is phosphorylated to phenylphosphate by
177 phenylphosphate synthase (Proteins 1 and 2) before the carboxylation, facilitated by an
178 accessory protein (Protein 3) (50-52). Subsequently, the core enzyme composed of
179 α, β, and γ components catalyzing the carboxylation using CO_2 as a substrate and the δ
180 subunit catalyzing the dephosphorylation are involved in converting phenylphosphate
181 into 4-hydroxybenzoic acid via phenolate anion (57-59). Based on the above, AV
182 carboxylation in SYK-6 was expected to proceed as follows. i) Putative 4-acetyl-2-
183 methoxyphenylphosphate (AVP) synthetase encoded by SLG_06540 and SLG_06530
184 phosphorylates AV. ii) Putative phosphatase encoded by SLG_06490 dephosphorylates
185 the phosphorylated AV. iii) Putative biotin-dependent carboxylase encoded by
186 SLG_06520, SLG_06510, and SLG_06500 carboxylates the AV dephosphorylated
187 anion intermediate.
188 Reverse transcription (RT)-polymerase chain reaction (PCR) analysis was
189 conducted using total RNA prepared from the SYK-6 cells grown in the presence of AV
190 to examine whether SLG_06540–SLG_06490 form a transcription unit. Specific

191 amplification was observed from SLG_06540 to SLG_06490, indicating that
192 SLG_06540–SLG_06490 form an operon (Fig. 1B and C).
193
194 **Roles of SLG_06540–SLG_06490 in AV and AS catabolism.** To examine whether
195 SLG_06540−SLG_06490 are involved in AV catabolism in SYK-6, disruption mutants
196 of SLG_06540−SLG_06490 (Δ06540–Δ06490) were created via homologous
197 recombination (Fig. S3). The growth of Δ06540–Δ06490 cells on AV was evaluated.
198 Since SYK-6 cannot grow at a concentration of several millimolar of AV, 1 mM AV was
199 added to the Wx medium at the beginning of cultivation, and another 1 mM AV was
200 added after 52 h of incubation. The OD_{660} of SYK-6 increased after 20 h of cultivation,
201 and further growth was observed when AV was added after 52 h. In contrast, all mutants
202 completely lost their capacity to grow on AV (Fig. S4A). Additionally, each mutant also
203 completely lost the capacity to grow on AS (Fig. S4B). These results indicate that
204 SLG_06540–SLG_06490 are essential for AV and AS catabolism; thus, we designated
205 these genes *acvA–acvF*.
206
207 **SLG_06550 is the transcriptional regulator of *acvABCDEF*.** SLG_06550,
208 located just upstream of *acvA*, showed 25% amino acid sequence identity with NphR,
209 an AraC-type transcriptional regulator that positively regulates the 4-nitrophenol
210 monooxygenase gene (*nphA1A2*) of *Rhodococcus* sp. strain PN1 (60). To examine
211 whether SLG_06550 is involved in the transcriptional *acvABCDEF* regulation in SYK-
212 6, an SLG_06550 disruption mutant (Δ06550) was created and its capacity to grow on

213 Wx medium containing AV was examined (Fig. S5A and B). Δ06550 completely lost its
214 capacity to grow on AV (Fig. S5C), suggesting that SLG_06550 positively regulates the
215 *acvABCDEF* operon, and this gene was named *acvR*.
216
217 ***acvABCDEF* confers a host strain the capacity to carboxylate AV and AS.** To
218 examine whether *acvABCDEF* encodes the AV and AS carboxylase system, a plasmid
219 carrying *acvABCDEF* in pJB861 was introduced into a host strain, *Sphingobium*
220 *japonicum* UT26S, which is incapable of AV and AS conversion. The UT26S genome
221 contains genes that show 32% (SJA_C1-33200) and 50% (SJA_C1-33210) amino acid
222 sequence identity with *acvC* and *acvD,* encoding putative BCCP and BC, respectively,
223 but no ortholog of *acvA* and *acvB* (encoding putative AVP synthetase), *acvE* (encoding
224 putative CT), and *acvF* (encoding putative phosphatase). The resting cells of UT26S
225 expressing *acvABCDEF* [optical density at 600 nm (OD_{600}) = 10.0] were incubated with
226 200 μM AV for 1 h. HPLC–MS analysis showed that VAA was produced (Fig. 3A–D).
227 When the same resting cells were incubated with 200 μM AS for 4 h, compound III
228 with a retention time of 3.4 min was produced (Fig. 3E and F). Negative electrospray
229 ionization-MS (ESI-MS) analysis of compound III showed a major fragment at *m/z* 239
230 (Fig. 3G and H), suggesting that compound III was SAA (MW, 240). These results
231 indicate that *acvABCDEF* encodes components of the carboxylase system required for
232 AV and AS catabolism.
233
234 **A mixture of AcvA and AcvB catalyzes the phosphorylation of AV and AS.**

Proteins 1 and 2 (phenylphosphate synthase) of *T. aromatica* K172, where *acvA* and *acvB,* respectively, show amino acid sequence similarity, convert phenol to phenylphosphate by the coexistence of both (51). MgATP is essential as a phosphoryl donor for this conversion and Mn^{2+} promotes catalytic activity (51). Each *acvA* and *acvB* fused with a His-tag at the 5' terminus was expressed in *E. coli* to characterize the function of *acvA* and *acvB.* Sodium dodecyl sulfate-polyacrylamide gel electrophoresis (SDS-PAGE) analysis showed the production of 71-kDa and 40-kDa proteins in cell extracts of *E. coli* expressing His-tagged *acvA* and *acvB,* respectively (Fig. S6).

Crude AcvA (500 μg/mL), AcvB (500 μg/mL), and AcvA + AcvB (500 μg/mL each) reacted with 200 μM AV, respectively, in the presence of 2 mM ATP, 2 mM $MgCl_2$, and 200 μM $MnCl_2$. HPLC–MS analysis showed that AV was completely converted into compound IV (1.9 min) after 30 min of incubation when AcvA and AcvB coexisted (Fig. 4A–C). Negative ESI-MS analysis of compound IV showed a fragment at *m*/*z* 245. Compound IV was identified as AVP (MW, 246) based on the molecular weight deduced from the fragment ion (Fig. 4D and E). Therefore, it was suggested that AcvAB phosphorylated the hydroxy group of AV.

AcvA and AcvB were purified to near homogeneity by Ni affinity chromatography from the cell extracts of *E. coli* expressing His-tagged *acvA* and *acvB*, respectively (Fig. S6). However, because the specific activity of purified AcvA + AcvB was lower than that of crude AcvA + AcvB, the AcvAB enzyme properties were investigated using crude enzymes.

To examine the AcvAB cofactor requirement, crude AcvA + AcvB (50–1000 μg

257 protein/mL each) was incubated with 100 μM AV in the presence and absence of
258 cofactors (2 mM ATP, 2 mM $MgCl_2$, 200 μM $MnCl_2$, 2 mM ATP + 2 mM $MgCl_2$, 2 mM
259 ATP + 200 μM $MnCl_2$, 2 mM $MgCl_2$ + 200 μM $MnCl_2$, and 2 mM ATP + 2 mM $MgCl_2$
260 + 200 μM $MnCl_2$). The highest activity (ca. 111 nmol·min^{-1}·mg^{-1}) was obtained in the
261 presence of ATP + Mg^{2+} + Mn^{2+}, whereas 42% and 3% activities were observed with
262 ATP + Mg^{2+} and ATP + Mn^{2+}, respectively. No activity was observed in the presence of
263 the other cofactors. These results indicate that AcvAB used MgATP as a phosphoryl
264 donor for AV phosphorylation similar to the phenylphosphate synthase of *T. aromatica*
265 K172, and that phosphorylation activity is promoted in the presence of Mn^{2+}.
266 Crude AcvA + AcvB (10–500 μg protein/mL each) was incubated with 100 μM AV,
267 AS, acetophenone, 4'-hydroxyacetophenone, 3'-hydroxyacetophenone, 3',4'-
268 dihydroxyacetophenone, 3'-hydroxy-4'-methoxyacetophenone, 3',4'-
269 dimethoxyacetophenone, 3',4',5'-trimethoxyacetophenone, 4'-hydroxypropiophenone,
270 4'-hydroxybuthyrophenone, 4'-hydroxyvalerophenone, guaiacol, vanillic acid, and 4-
271 hydroxybenzoic acid, respectively, in the presence of 2 mM ATP + 2 mM $MgCl_2$ + 200
272 μM $MnCl_2$ to examine the substrate range of AcvAB (Fig. S7). HPLC–MS analysis
273 showed that AcvAB converted AS into 4-acetyl-2,6-dimethoxyphenylphosphate (ASP)
274 (Fig. S8A–C). AcvAB exhibited activity toward compounds with the hydroxy group at
275 the 4-position of the aromatic ring except for vanillic acid and 4-hydroxybenzoic acid
276 (Fig. S8). AcvAB also showed activity toward 3'-hydroxyacetophenone but it showed
277 no activity toward 3'-hydroxy-4'-methoxyacetophenone.
278

279 **AcvF catalyzes the dephosphorylation of AVP and ASP.** Because AcvF showed
280 23% amino acid sequence identity with NagD of *E. coli* K-12, belonging to the HAD
281 superfamily, including phosphatases, AcvF is expected to have dephosphorylation
282 activities for AVP and ASP. (56). The AcvF function was characterized by expressing
283 *acvF* fused with a His-tag at the 5' terminus in *E. coli*. SDS-PAGE analysis showed a
284 32-kDa protein production in cell extract of *E. coli* expressing His-tagged *acvF*, and
285 AcvF was purified to near homogeneity by Ni affinity chromatography (Fig. S6). To
286 investigate the AVP and ASP dephosphorylation ability of AcvF, AVP and ASP were
287 produced from AV and AS, respectively, using crude AcvA + AcvB. Crude AcvA +
288 AcvB (1 mg protein/mL each) was incubated with 200 μM AV and AS, respectively, in
289 the presence of 2 mM ATP + 2 mM $MgCl_2$ + 200 μM $MnCl_2$ for 2 h. HPLC analysis
290 confirmed that AV and AS were completely converted into AVP and ASP, respectively,
291 and the filtrate obtained via ultrafiltration (MW cutoff, 10 kDa) was used as substrates.
292 Purified AcvF (5 μg protein/mL) was incubated with 100 μM AVP or ASP for 60 min.
293 HPLC analysis of the reaction mixtures showed that AcvF converted AVP into AV (Fig.
294 5A and B). Similarly, AcvF converted ASP into AS (Fig. 5C and D). These results
295 indicated that AcvAB phosphorylates AV and AS, which is then dephosphorylated by
296 AcvF, respectively.
297
298 **Carboxylation of AV and AS by a mixture of AcvAB, AcvF, and AcvCDE.** It
299 was expected that AcvC-AcvD-AcvE could carboxylate the acetyl groups of AV and AS
300 since *acvC*, *acvD*, and *acvE* was predicted to encode biotin-dependent carboxylase

components, BCCP, BC, and CT, respectively (61). A His-tag was fused to the 5' terminus of *acvC* to express *acvCDE* in *E. coli*, characterizing the function of *acvC*, *acvD*, and *acvE*. However, SDS-PAGE analysis showed no clear AcvD and AcvE production, except for AcvC (Fig. S9). Furthermore, the resulting cell extract of *E. coli* expressing *acvCDE* (1 mg protein/mL) was incubated with 100 μM AV in the presence of crude AcvA + AcvB (1 mg protein/mL each), purified AcvF (10 μg protein/mL), 2 mM ATP + 2 mM $MgCl_2$ + 200 μM $MnCl_2$, and 10 mM $NaHCO_3$ for 60 min; however, no reaction product was observed (data not shown). Therefore, *acvCDE* was expressed under the control of the Q5 promoter of the pQF vector using *Sphingobium japonicum* UT26S as a host. The resulting cell extract of UT26S expressing *acvCDE* (crude AcvCDE) reacted with 100 μM AV under the same reaction conditions as above. The conversion product was undetected when the cell extract of UT26S harboring pQF vector was used (Fig. 6A and B), whereas VAA was detected in the reaction with crude AcvCDE (Fig. 6C). Additionally, SAA was detected when AS was used as a substrate (Fig. 6D–F). These results suggest that AcvCDE catalyzes AV and AS carboxylation.

To examine whether AcvCDE directly carboxylates AV, crude AcvCDE (1 mg protein/mL) was incubated with 100 μM AV in the presence of 2 mM ATP + 2 mM $MgCl_2$ + 200 μM $MnCl_2$, and 10 mM $NaHCO_3$ for 60 min, but no VAA formation was observed (Fig. S10A and B). Conversely, when AVP was used as a substrate, VAA was generated under the same reaction condition except for the substrate (Fig. S10C and D). These results indicate that AcvCDE could not directly carboxylate AV. Although *acvF* is essential for SYK-6 growth on AV, crude AcvCDE converted AVP into VAA in the

absence of AcvF. When AVP was incubated with a cell extract of UT26S harboring pQF, conversion of AVP into AV was shown (Fig. S10E). Therefore, enzyme(s) present in UT26S appear to complement the AcvF function.

Expression of *acvABCDEF* with *vceA*, *vceB*, and *aroY* in *Pseudomonas* sp. NGC703 enables ccMA production from AV. Our previous study demonstrated ccMA production from vanillic acid using *Pseudomonas* sp. NGC703 [a mutant of *Pseudomonas* sp. NGC7 deficient in the protocatechuic acid 3,4-dioxygenase gene (*pcaHG*) and ccMA cycloisomerase gene (*catB*)] cells harboring pTS084, comprising the protocatechuic acid decarboxylase (*aroY*), flavin prenyltransferase (*kpdB*), vanillic acid *O*-demethylase (*vanAB*), and catechol 1,2-dioxygenase (*catA*) genes (Fig. 7A) (34). This study examined whether ccMA production from AV is possible using NGC7 as a platform.

We constructed pSEVA*acv* (RO1600/ColE1 *ori*), which carries *acvABCDEF* under the control of the *lac* promoter, and introduced pSEVA*acv* into NGC7. When resting cells of NGC7(pSEVA*acv*) (OD_{600} = 10.0) were incubated with 200 μM AV, AV was converted into VAA (Fig. S11A and B). In our previous study, we found VceA, which converts VAA and SAA into vanilloyl-CoA and syringoyl-CoA, respectively, and VceB, which converts vanilloyl-CoA and syringoyl-CoA into vanillic acid and syringic acid, respectively, from SYK-6, and that VAA can be converted into vanillic acid by these enzymes (Fig. 7A) (5). Thus, we constructed pTS093*vce* (RK2 *ori*), which carries *vceA* and *vceB* under the control of the *lac* promoter, and introduced pTS093*vce* into

345 NGC7(pSEVA*acv*). When resting cells of NGC7(pSEVA*acv* + pTS093*vce*) (OD_{600} =
346 10.0) were incubated with 200 μM AV, AV was converted to vanillic acid (Fig. S11C).
347 To produce ccMA from AV, we constructed pTS093*vce-aroY* (RK2 *ori*), which carries
348 *aroY* with *vceA* and *vceB* under the control of the *lac* promoter, and then introduced
349 pTS093*vce-aroY* into NGC703 with pSEVA*acv* (Fig. 7B). When the resulting strain was
350 grown on an MMx-3 medium [34.2 g/L $Na_2HPO_4 \cdot 12H_2O$, 6.0 g/L KH_2PO_4, 1.0 g/L
351 NaCl, 2.5 g/L $(NH_4)_2SO_4$, 490 mg/L $MgSO_4 \cdot 7H_2O$, 14.7 mg/L $CaCl_2 \cdot 2H_2O$, and 5 mg/L
352 $FeSO_4 \cdot 7H_2O$] containing 15 g/L glucose as a carbon source, 1.2 mM AV could be
353 converted into ccMA with 96% yield (mol ccMA/mol AV) (Fig. 7C). These results
354 demonstrate that combining *acvABCDEF* with *vceA* and *vceB* is useful for the value-
355 added chemical production from AV, a major aromatic monomer produced in
356 oxidative/base-catalyzed lignin depolymerization.
357

DISCUSSION

AV and AS are major lignin-derived aromatic monomers produced in alkaline oxidative depolymerization (13-16) and base-catalyzed depolymerization of lignin (17-19, 62-68). They are also contained in the black liquor produced during the kraft pulping process (20). This study identified *acvABCDEF* that encodes AV and AS carboxylase components and showed that these genes help produce value-added chemicals from AV.

As phenylphosphate synthases, Proteins 1 and 2 of *T. aromatica* K172 (51), $PpsAB_{GM}$ of *Geobacter metallireducens* ATCC 53774 (69), and $PpsAB_{FP}$ of *Ferroglobus placidus* DSM 10642 (70) have been reported. These enzymes are responsible for producing a phosphorylated intermediate essential for phenol carboxylation. Although not an example of carboxylation, 4-methylbenzyl phosphate synthase (CreHI) from *Corynebacterium glutamicum* produces a phosphorylated intermediate essential for oxidizing the 4-cresol methyl group (71). Based on the amino acid sequence similarity, AcvA corresponds to Protein 1, $PpsA_{GM}$, $PpsA_{FP}$, and CreH (40%–44% amino acid sequence identity), while AcvB corresponds to Protein 2, $PpsB_{GM}$, $PpsB_{FP}$, and CreI (39%–42% amino acid sequence identity) (Table S2). Among these phenylphosphate synthases, the reaction mechanism has been proposed in Proteins 1 and 2 of *T. aromatica* K172 (52). The phenol phosphorylation by Proteins 1 and 2 is similar to the ping-pong mechanism proposed for phosphoenolpyruvate synthase and is thought to proceed by the following two-step reactions. i) Protein 2 transfers the phosphoryl group from MgATP to His569 of Protein 1, producing His569-β-phosphate-

γ-phosphate. ii) The terminal γ-phosphate is irreversibly hydrolyzed from Protein 1, and then the phosphate group of His569-β-phosphate is transferred to phenol to form phenylphosphate. AcvB, Protein 2, $PpsB_{GM}$, $PpsB_{FP}$, and CreI have an ATP binding domain (PPDK_N; PF01326) (Fig. S12). Additionally, AcvA, $PpsA_{GM}$, $PpsA_{FP}$, and CreH contained a His residue corresponding to Protein 1 His569 (Fig. S13). These facts suggest that AcvAB, $PpsAB_{GM}$, $PpsAB_{FP}$, and CreHI phosphorylate the hydroxy group of each substrate by a mechanism common to Proteins 1 and 2 of *T. aromatica* K172.

AcvF dephosphorylated AVP and ASP produced from AV and AS, respectively. In *T. aromatica* K172, phenylphosphate produced by Proteins 1 and 2 is dephosphorylated by the δ subunit of phenylphosphate carboxylase or non-enzymatic reaction generating phenolate anion. This intermediate is used as a substrate for carboxylation by the core enzyme [$(\alpha\beta\gamma)_3$] of phenylphosphate carboxylase (57, 58). Although AcvF and the δ subunit of phenylphosphate carboxylase have no significant similarity with each other (7% identity), both AcvF and the δ subunit are classified in the HAD-like superfamily. Relatively low overall sequence similarity has been reported for this superfamily of enzymes (72). Therefore, AcvF probably dephosphorylates AVP/ASP, similar to the phenylphosphate carboxylase δ subunit, producing an anionic intermediate for AV/AS.

Crude AcvCDE converted AVP into VAA (Fig. S10C and D). This result suggests that phosphatase(s) present in UT26S complemented the AcvF function. Since *acvF* is essential for SYK-6 growth on AV/AS, the dephosphorylation of AVP/ASP catalyzed by AcvF appears crucial for AV/AS carboxylation. To verify this, AcvCDE purification and functional analysis using the purified enzyme are necessary for the future.

AcvC, AcvD, and AcvE were predicted to be BCCP, BC, and CT, respectively, based on the amino acid sequence similarity. In addition to these components, biotin-dependent carboxylases require biotin-protein ligase (BPL), which specifically adds biotin to a lysine residue of BCCP (73). A search for putative BPL genes in SYK-6 revealed the presence of SLG_23040, which showed 23% amino acid sequence identity with BirA of *B. subtilis* 168 (74). AVP was converted to VAA via *acvCDE* expression in *S. japonicum* UT26S, suggesting that AcvC (BCCP) was biotinylated by BPL present in UT26S. SJA_C1-13370, which showed 44% amino acid sequence identity with SLG_23040, may have functioned as BPL. *xccA*, *xccC*, and *xccB*, encoding putative biotin-dependent carboxylase components of *A. aromaticum* EbN1, are thought to be involved in 4'-hydroxyacetophenone carboxylation, which is structurally similar to AV (55). Additionally, *apkA-apkB-apkC*, encoding putative biotin-dependent carboxylase components of *R. rhodochrous* GD02, were recently predicted to be involved in AV catabolism (20). However, these enzyme genes have not been functionally characterized. To the best of our knowledge, this is the first report demonstrating that biotin-dependent carboxylase is involved in the catabolism of aromatic compounds. Phenol carboxylase of *T. aromatica* K172 (50-52, 57-59, 75) and acetophenone carboxylase [Apc($\alpha\alpha'\beta\gamma$)$_2$ core complex and Apcε] of *A. aromaticum* EbN1 (76, 77) are not biotin-dependent enzymes and show no similarity to AcvC, AcvD, and AcvE. Altogether, AV/AS carboxylation in SYK-6 seems to proceed as follows (Fig. S14). i) AV/AS is converted into AVP/ASP by transferring the phosphate group from MgATP to the hydroxy group of AV/AS by AcvAB. ii) AcvF dephosphorylates the resulting

AVP/ASP to produce an anionic intermediate. iii) The anionic intermediate is converted to VAA/SAA by transferring the carboxyl group from the carboxylated biotin by AcvCDE.

In SYK-6, AV/AS is converted to VAA/SAA, an intermediate metabolite in the β-aryl ether catabolism (Fig. 1). Therefore, we investigated whether β-aryl ether catabolic genes and AV/AS catabolic genes coexist in the genomes of *Altererythrobacter* sp. strain Root672, *Altererythrobacter atlanticus* 26DY36, *Erythrobacter* sp. strain SG61-1L, *Sphingobium* sp. strain 66-54, and *Sphingobium* sp. strain B12D2A, which have orthologs of the β-aryl ether catabolic genes (Table S3). Orthologs of *acvABCDEF* showing more than 45% amino acid sequence identity were found in all strains. Particularly, the gene order of *acvABCDEF* in *Altererythrobacter atlanticus* 26DY36, *Sphingobium* sp. 66-54, and *Sphingobium* sp. B12D2A was conserved. Therefore, these strains may have evolved an AV/AS catabolic pathway by connecting the AV/AS carboxylase and the downstream pathway enzymes of the β-aryl ether catabolism.

Finally, we successfully achieved the microbial AV conversion (1.2 mM) into ccMA with 96% yield (mol ccMA/mol AV) using *Pseudomonas* sp. NGC703(pSEVA*acv* + pTS093*vce-aroY*), which is a *pcaHG catB* NGC7 mutant carrying *acvABCDEF*, *vceA*, *vceB*, and *aroY* (Fig. 7) (5, 34). In producing value-added chemicals from lignin through biological funneling, it is necessary to convert all degradation products obtained by chemical depolymerization of lignin or to degrade compounds that cannot be converted into products and not leave them in the culture medium to facilitate product purification. The results of this study will provide

446 invaluable insights for improving the yield and purity of products in the biological
447 conversion of aromatics obtained by alkaline oxidative and base-catalyzed
448 depolymerization of lignin.

MATERIALS AND METHODS

Bacterial strains, plasmids, and culture conditions. The strains and plasmids used in this study are listed in Table 1. *Sphingobium* sp. strain SYK-6 and its mutants were grown in lysogeny broth (LB), Wx-SEMP, and Wx-SEMP containing 5 mM AV at 30°C. *Sphingobium japonicum* UT26S, *Pseudomonas* sp. NGC7, and its mutants were grown in LB at 30°C. When necessary, 12.5 mg/L nalidixic acid, 100 mg/L streptomycin, 25–50 mg/L kanamycin, or 12.5–15.0 mg/L tetracycline was added to the cultures. *Escherichia coli* strains were grown in LB at 37°C. For cultures of cells carrying antibiotic resistance markers, the media for *E. coli* transformants were supplemented with 100 mg/L ampicillin, 25 mg/L kanamycin, or 12.5 mg/L tetracycline.

Preparation of substrates. VAA and SAA were prepared as described previously (5). For the preparation of AVP and ASP, AV or AS (final concentration: 200 μM) was incubated in 1 mL 50 mM Tris-HCl buffer (pH 7.5; Buffer A) containing the cell extracts of *E. coli* BL21(DE3) cells harboring pE16*acvA* and *E. coli* BL21(DE3) cells harboring pE16*acvB* (1 mg protein/mL each), 2 mM ATP, 2 mM $MgCl_2$, and 200 μM $MnCl_2$. After incubation for 2 h at 30°C, complete consumption of AV or AS was confirmed by HPLC, and then the reaction mixtures were filtered using an Amicon Ultra spin filter unit (10 kDa cutoff; Millipore). *Cis*,*trans*-muconic acid was prepared by incubating ccMA (1.0 g/L) for 2 h at 60°C in a solution whose pH was adjusted to 4.0 with acetic acid. After the incubation, the pH was adjusted to 7 with sodium hydroxide and it was stored at -80°C until use. Other aromatic compounds were purchased from

Tokyo Chemical Ind., Co., Ltd.; Sigma-Aldrich Co., LLC.; and FUJIFILM Wako Pure Chemical Corporation.

Identification of the metabolites. SYK-6 cells grown in LB were inoculated into Wx-SEMP to an OD_{600} of 0.2 and grown at 30°C. AV (5 mM) was added when the OD_{600} of the culture reached 0.5, and the culture was then further incubated for 12 h. Cells were collected by centrifugation (5,000 × *g* for 5 min at 4°C), washed twice with Wx minimal medium, and resuspended in the same medium. The resultant cell suspensions were inoculated into Wx medium containing 1 mM AV to an OD_{600} of 0.2 and incubated for 33 h at 30°C. The reaction mixtures were centrifuged, and the supernatants were collected. The resulting filtered samples were analyzed by HPLC–MS.

HPLC–MS analysis. HPLC–MS analysis was performed with the Acquity UPLC system coupled with an Acquity TQ detector as described previously (78). The in vivo reaction products of AV and AS were analyzed using a UPLC equipped with an Acquity UPLC BEH C18 column (2.1 by 100 mm; Waters). The flow rate of the mobile phase was 0.5 mL/min. The in vitro reaction products of AV, AS, acetophenone, 4'-hydroxyacetophenone, 3'-hydroxyacetophenone, 3',4'-dihydroxyacetophenone, 3'-hydroxy-4'-methoxyacetophenone, 3',4'-dimethoxyacetophenone, 3',4',5'-trimethoxyacetophenone, 4'-hydroxypropiophenone, 4'-hydroxybuthyrophenone, 4'-hydroxyvalerophenone, guaiacol, vanillic acid, 4-hydroxybenzoic acid, AVP, and ASP

493 were analyzed using a UPLC equipped with a TSKgel ODS-140HTP column (2.1 by
494 100 mm; Tosoh). The flow rate of the mobile phase was 0.5 mL/min. The mobile phase
495 was a mixture of Solution A (acetonitrile containing 0.1% formic acid) and Solution B
496 (water containing 0.1% formic acid) with the following conditions: *(i) detection of in*
497 *vivo reaction products of AV*: 0 to 3.0 min, linear gradient from 5 to 15% A; 3.0 to 4.0
498 min, decreasing gradient from 15 to 5% A. *(ii) detection of in vivo reaction products of*
499 *AS*: 0 to 3.5 min, 10% A; 3.5 to 4.0 min, linear gradient from 10 to 30% A; 4.0 to 5.0
500 min, 30% A; 5.0 to 5.1 min, decreasing gradient from 30 to 10% A; 5.1 to 6.0 min, 10%
501 A. *(iii) detection of the in vitro reaction products*: 0 to 0.5 min, 2% A; 0.5 to 1.5 min,
502 linear gradient from 2 to 15% A; 1.5 to 3.0 min, linear gradient from 15 to 100% A; 3.0
503 to 4.0 min, decreasing gradient from 100 to 2% A; 4.0 to 5.0 min, 2% A. AV, AS,
504 acetophenone, 4'-hydroxyacetophenone, 3'-hydroxyacetophenone, 3',4'-
505 dihydroxyacetophenone, 3'-hydroxy-4'-methoxyacetophenone, 3',4'-
506 dimethoxyacetophenone, 3',4',5'-trimethoxyacetophenone, 4'-hydroxypropiophenone,
507 4'-hydroxybuthyrophenone, 4'-hydroxyvalerophenone, guaiacol, vanillic acid, 4-
508 hydroxybenzoic acid, AVP, ASP, VAA, and SAA were detected at 275, 300, 255, 275,
509 260, 275, 274, 274, 280, 271, 272, 271, 276, 260, 255, 303, 300, 280, and 308 nm,
510 respectively. In the ESI-MS analysis, MS spectra were obtained using the negative-ion
511 and positive-ion modes with the settings reported in our previous study (78).
512
513 **Resting cell assay.** SYK-6 cells grown in LB were inoculated into Wx-SEMP to an
514 OD_{600} of 0.2 and grown at 30°C until the OD_{600} of the culture reached 0.5. Following

515 the addition of 5 mM AV, the cells were incubated for a further 12 h as the inducing
516 condition. For the non-inducing condition, the culture was incubated for a further 12 h
517 without AV. The cells were collected by centrifugation (5,000 × *g* for 5 min at 4°C) and
518 then washed twice with Buffer A. The cells were resuspended in the same buffer and
519 used as resting cells. Preparation of resting cells of *S. japonicum* UT26S are described
520 below.

521 Resting cells of SYK-6 (OD_{600} of 5.0) were incubated with 1.0 mM AV at 30°C
522 with shaking. Resting cells of UT26S harboring pJB861and UT26S harboring pJB*acv*
523 (OD_{600} of 10.0) were incubated with 200 μM AV or AS at 30°C with shaking. Portions
524 of the reaction mixtures were collected, and the amounts of compounds were measured
525 by HPLC.

526

527 **Analysis of nucleotide and amino acid sequences.** Nucleotide sequences were
528 determined by Eurofins Genomics. Sequence analysis was performed using the
529 MacVector program (MacVector, Inc.). Sequence similarity searches, pairwise
530 alignments, and multiple alignments were conducted using the BLASTP program (79),
531 the EMBOSS Needle program through the EMBL-EBI server (80), and the Clustal
532 Omega program (81), respectively.

533

534 **RT-PCR analysis.** SYK-6 cells grown in LB were inoculated into Wx-SEMP to an
535 OD_{600} of 0.2 and grown at 30°C. AV (5 mM) was added when the OD_{600} of the culture
536 reached 0.5, and the culture was then further incubated for 6 h. Total RNA was isolated

537 from the cells using an Illumina RNAspin Mini RNA isolation kit (GE Healthcare). The
538 samples were treated with DNase I to remove any contaminating genomic DNA. Total
539 RNA (4 μg) was reverse transcribed using SuperScript IV reverse transcriptase
540 (Invitrogen) with random hexamer primers. The cDNA was purified using a NucleoSpin
541 Gel and PCR Clean-up kit (Takara Bio, Inc.). PCR was performed with the cDNA,
542 specific primers (Table 2), and Q5 High-Fidelity DNA Polymerase (New England
543 Biolabs). The DNA obtained was electrophoresed on a 0.8% agarose gel.
544
545 **Construction of mutants.** To construct the mutants, the upstream and downstream
546 regions (0.7–1.0 kb each) of the genes were amplified by PCR from SYK-6 total DNA
547 using the primer pairs listed in Table 2. The amplified fragments were ligated into
548 pAK405 (Kaczmarczyk et al., 2012). Each of the resulting plasmids was introduced into
549 SYK-6 cells by triparental mating, and the resulting mutants were selected as described
550 previously (82). Disruption of each gene was examined by Southern hybridization
551 analysis using the digoxigenin system (Roche) or colony PCR using the primer pairs
552 listed in Table 2.
553
554 **Growth measurement.** SYK-6 and its mutant cells grown in LB were inoculated
555 into Wx-SEMP to an OD_{600} of 0.2 and grown at 30°C. AV (5 mM) was added when the
556 OD_{600} of the culture reached 0.5, and the culture was then further incubated for 12 h.
557 Cells were collected by centrifugation (5,000 × *g* for 5 min at 4°C), washed twice with
558 Wx minimal medium, and resuspended in the same medium. The resultant cell

559 suspensions were inoculated into Wx medium containing 1 mM AV or AS to an OD_{660}
560 of 0.2. Cells were incubated at 30°C with shaking (60 rpm) and cell growth was
561 monitored every hour by measuring the OD_{660} with a TVS062CA biophotorecorder
562 (Advantec Co., Ltd.). After 52 h (AV) and 48 h (AS) cultivation, 1 mM AV or AS was
563 added to the culture medium.
564
565 **Expressions of *acvABCDEF* in heterologous hosts and enzyme purification.** For
566 expression of *acvABCDEF* in *S. japonicum* UT26S, a 7.4-kb fragment carrying
567 *acvABCDEF* with the NotI site at 5' terminus and 3' terminus was amplified by PCR.
568 The amplified fragment was cloned into the BamHI site of pET-21a(+) using In-Fusion
569 HD cloning Kit (Takara Bio), and the NotI fragment of the resulting plasmid was then
570 inserted in pJB861 to generate pJB*acv*. For expression of *acvA*, *acvB*, *acvF*, and
571 *acvCDE* in *E. coli*, DNA fragments carrying each gene were amplified by PCR from the
572 SYK-6 total DNA using primer pairs shown in Table 2. The amplified fragments were
573 cloned into NdeI and BamHI sites of pET-16b using In-Fusion HD cloning Kit. For
574 expression of *acvCDE* in UT26S, DNA fragment carrying *acvCDE* was amplified by
575 PCR from the SYK-6 total DNA (Table 2). The amplified fragment was cloned into
576 BamHI site of pQF using an NEBuilder HiFi DNA assembly cloning kit (New England
577 Biolabs) to generate pQF*acvCDE*. Nucleotide sequences of the resultant plasmids were
578 then confirmed.
579 pJB*acv* and pQF*acvCDE* were introduced into UT26S cells by electroporation.
580 Cells of UT26S harboring pJB*acv* were inoculated into LB supplemented with 1 mM *m*-

toluic acid as an inducer and grown at 30°C for 24 h. Cells of UT26S harboring pQF*acvCDE* were inoculated into LB supplemented with 0.1 mM 4-isopropylbenzoic acid as an inducer and grown at 30°C for 24 h. Cells of *E. coli* BL21(DE3) harboring pE16*acvA*, pE16*acvB*, pE16*acvF*, or pE16*acvCDE* were grown in LB at 30°C. Each gene expression was induced for 4 h at 30°C by adding 1 mM isopropyl-β-D-thiogalactopyranoside when the OD_{600} of the culture reached 0.5. The cells of UT26S and *E. coli* transformants were then collected by centrifugation (5,000 × *g* for 5 min at 4°C), washed twice with buffer A, resuspended in the same buffer, and used as resting cells. The cells were then disrupted using an ultrasonic disintegrator. After centrifugation (19,000 × *g* for 15 min at 4°C), the supernatants were obtained as cell extracts (crude enzymes). AcvA, AcvB, and AcvF were purified from cell extracts of *E. coli*(pE16*acvA*), *E. coli*(pE16*acvB*), and *E. coli*(pE16*acvF*), respectively, using a His SpinTrap column (GE Healthcare). Resultant elution fractions were subjected to desalting and concentration using an Amicon Ultra centrifugal filter unit (30 kDa cutoff; Merck Millipore), and the enzyme preparations were stored at -80°C. SDS-PAGE and protein concentration determination using the Bradford method were performed as described previously (43).

Enzyme activity of AcvAB. Crude AcvA, crude AcvB, crude AcvA + AcvB (500 µg protein/mL each) or purified AcvA + AcvB (100 µg protein/mL each) were incubated with 100 or 200 µM AV in the presence of 2 mM ATP, 2 mM $MgCl_2$, and 200 µM $MnCl_2$ in buffer A for 10–30 min at 30°C. The reactions were stopped by adding

603 acetonitrile to a final concentration of 50%. Protein precipitates were removed through
604 centrifugation (19,000 × *g* for 15 min). The resulting supernatants were diluted with
605 water to a final concentration of acetonitrile of 25%, filtered, and analyzed using
606 HPLC–MS. Specific activity was expressed in moles of AV converted per minute per
607 milligram of protein.
608
609 **Enzyme properties of AcvAB.** The enzyme reaction was conducted by incubating
610 crude AcvA + AcvB (10–1000 μg protein/mL each) with 200 μM AV, 2 mM ATP, 2 mM
611 $MgCl_2$, and 200 μM $MnCl_2$ in buffer A for 10 min at 30°C. After incubation, the
612 amounts of AV were measured using HPLC. To examine cofactor requirement of
613 AcvAB, crude AcvA + AcvB (50–1000 μg protein/mL each) was incubated with
614 100 μM AV in the presence and absence of cofactors (2 mM ATP, 2 mM $MgCl_2$, 200
615 μM $MnCl_2$, 2 mM ATP + 2 mM $MgCl_2$, 2 mM ATP + 200 μM $MnCl_2$, 2 mM $MgCl_2$ +
616 200 μM $MnCl_2$, and 2 mM ATP + 2 mM $MgCl_2$ + 200 μM $MnCl_2$) for 10 min at 30°C.
617 To determine the substrate range, 100 μM AV, AS, acetophenone, 4'-
618 hydroxyacetophenone, 3'-hydroxyacetophenone, 3',4'-dihydroxyacetophenone, 3'-
619 hydroxy-4'-methoxyacetophenone, 3',4'-dimethoxyacetophenone, 3',4',5'-
620 trimethoxyacetophenone, 4'-hydroxypropiophenone, 4'-hydroxybuthyrophenone, 4'-
621 hydroxyvalerophenone, guaiacol, vanillic acid, and 4-hydroxybenzoic acid were used
622 for the reaction, and the conversion of substrates and generation of reaction products
623 were analyzed using HPLC–MS.
624

625 **Enzyme activity of AcvF.** Purified AcvF (5 μg protein/mL) was incubated with
626 100 μM AVP or ASP in buffer A for 60 min at 30°C. The supernatants were then
627 analyzed using HPLC.
628
629 **Enzyme activity of AcvCDE.** Cell extract of *E. coli* BL21(DE3) harboring
630 pE16*acvCDE*, cell extract of *S. japonicum* UT26S harboring pQF, or cell extract of
631 UT26S harboring pQF*acvCDE* (1 mg protein/mL) was incubated with 100 μM AV or
632 AS, 2 mM ATP, 2 mM $MgCl_2$, 200 μM $MnCl_2$, and 10 mM $NaHCO_3$ in the presence or
633 absence of crude AcvA + AcvB (1 mg protein/mL each) and purified AcvF (10 μg
634 protein/mL) in buffer A for 60 min at 30°C. When using AVP as a substrate, cell extract
635 of UT26S harboring pQF or cell extract of UT26S harboring pQF*acvCDE* (1 mg
636 protein/mL) was incubated with 100 μM AVP, 2 mM ATP, 2 mM $MgCl_2$, 200 μM
637 $MnCl_2$, and 10 mM $NaHCO_3$ in buffer A for 60 min at 30°C. The supernatants were
638 then analyzed using HPLC.
639
640 **ccMA production from AV.** A 0.2-kb fragment carrying the *lac* promoter (P_{lac})
641 from pUC118 was amplified and cloned into the SfiI site of pSEVA241 (83) with In-
642 Fusion HD cloning kit to generate pSEVA241_P_{lac}. The 7.2-kb NotI fragment carrying
643 *acvABCDEF* from pJB*acv* was ligated into the corresponding site of pSEVA241_P_{lac} to
644 generate pSEVA*acv*. A 1.5-kb fragment carrying *vceA* and *vceB* was amplified by PCR
645 using pJHV01 (5) and the primer pairs listed in Table 2. The resulting fragment was
646 cloned into the BamHI site of pQF by NEBuilder HiFi DNA assembly cloning kit to

generate pQF*vce*. The 1.5-kb fragment carrying *vceA* and *vceB* was amplified by PCR using pQF*vce* and the primer pairs listed in Table 2. The resulting fragment was cloned into the EcoRI-XhoI site of pTS093 (12) with In-Fusion HD cloning kit to generate pTS093*vce*. The 1.6-kb KpnI fragment carrying *aroY* from pTS032 (35) was ligated into the corresponding sites of pTS093*vce* to generate pTS093*vce-aroY*. pSEVA241_P_{lac}, pSEVA*acv*, or pSEVA*acv* + pTS093*vce* was introduced into NGC7 cells by electroporation. pSEVA*acv* and pTS093*vce-aroY* were introduced into NGC703 (Δ*pcaHG catB*) cells by electroporation.

Conversion of AV by NGC7 transformants. Cells of NGC7 harboring pSEVA241_P_{lac}, NGC7 harboring pSEVA*acv*, and NGC7 harboring pSEVA*acv* + pTS093*vce* were grown in LB containing kanamycin or kanamycin + tetracycline for 16 h. The cells were collected by centrifugation at 9,000 × *g* for 3 min, washed twice with MMx-3 buffer [34.2 g/L $Na_2HPO_4{\cdot}12H_2O$, 6.0 g/L KH_2PO_4, 1.0 g/L NaCl, and 2.5 g/L $(NH_4)_2SO_4$], resuspended in the same buffer, and used as resting cells. Resting cells of NGC7 harboring pSEVA241_P_{lac}, NGC7 harboring pSEVA*acv*, and NGC7 harboring pSEVA*acv* + pTS093*vce* (OD_{600} of 10.0) were incubated with 200 μM AV or AS at 30°C with shaking. Portions of the reaction mixtures were periodically collected, and the reactions were stopped by centrifugation. The resultant supernatants were diluted, filtered, and analyzed using an HPLC instrument 1200 series (Agilent Technologies Inc.) equipped with a ZORBAX Eclipse Plus C18 column (4.6 by 150 mm; Agilent Technologies Inc.). The flow rate of the mobile phase was 1.0 mL/min, and the

669 detection wavelength was 280 nm. The mobile phase was a mixture of Solution A (50%
670 methanol containing 1% acetic acid) and Solution B (5% methanol containing 1% acetic
671 acid) with the following conditions: 0–8.0 min, linear gradient from 0% to 20% A; 8.0–
672 13.0 min, linear gradient from 20% to 100% A; 13.0–18.0 min, 100% A; 18.0–23.0 min,
673 decreasing gradient from 100% to 0% A; 23.0–25.5 min, 100% B.

674 Cells of NGC703(pSEVA*acv* + pTS093*vce-aroY*) were grown in LB containing
675 kanamycin and tetracycline for 16 h. The cells were collected by centrifugation at
676 9,000 × *g* for 3 min, washed twice with MMx-3 medium, and resuspended in 5 mL of
677 the same medium. The cells were then inoculated into 10 mL of MMx-3 medium
678 containing 15 g/L glucose, 1.2 mM AV, kanamycin, and tetracycline to an OD_{600} of 0.1
679 and incubated with shaking for 70 h at 30°C. Cell growth was measured by OD_{600}.
680 Portions of the cultures were periodically collected, and the reactions were stopped by
681 centrifugation. The resultant supernatants were diluted, filtered, and analyzed using a
682 HPLC instrument 1200 series. ccMA yields were calculated as [the produced ccMA
683 (mol)/the consumed AV (mol)] × 100%. The concentrations of glucose in the culture
684 were measured with a BF-5i biosensor (Oji Scientific Instruments, Ltd.).

685 **ACKNOWLEDGEMENT**

686 This work was supported by JST-Mirai Program Grant Number JPMJMI19E2,

687 Japan, a grant from the Ministry of Agriculture, Forestry and Fisheries of Japan (Rural

688 Biomass Research Project BM-D1310), and JSPS KAKENHI Grant Number

689 JP26850046.

690 # REFERENCES

691

692 1. Ragauskas AJ, Beckham GT, Biddy MJ, Chandra R, Chen F, Davis MF, Davison BH, Dixon RA, Gilna
693 P, Keller M, Langan P, Naskar AK, Saddler JN, Tschaplinski TJ, Tuskan GA, Wyman CE. 2014. Lignin
694 valorization: improving lignin processing in the biorefinery. Science 344:1246843.
695 2. Boerjan W, Ralph J, Baucher M. 2003. Lignin biosynthesis. Annu Rev Plant Biol 54:519–546.
696 3. Vanholme R, Demedts B, Morreel K, Ralph J, Boerjan W. 2010. Lignin biosynthesis and structure.
697 Plant Physiol 153:895–905.
698 4. Zakzeski J, Bruijnincx PCA, Jongerius AL, Weckhuysen BM. 2010. The catalytic valorization of lignin
699 for the production of renewable chemicals. Chem Rev 110:3552–3599.
700 5. Higuchi Y, Kato R, Tsubota K, Kamimura N, Westwood NJ, Masai E. 2019. Discovery of novel
701 enzyme genes involved in the conversion of an arylglycerol-β-aryl ether metabolite and their use in
702 generating a metabolic pathway for lignin valorization. Metab Eng 55:258-267.
703 6. Becker J, Wittmann C. 2019. A field of dreams: Lignin valorization into chemicals, materials, fuels,
704 and health-care products. Biotechnol Adv 37:107360.
705 7. Beckham GT, Johnson CW, Karp EM, Salvachúa D, Vardon DR. 2016. Opportunities and challenges
706 in biological lignin valorization. Curr Opin Biotechnol 42:40–53.
707 8. Borchert AJ, Henson WR, Beckham GT. 2021. Challenges and opportunities in biological funneling
708 of heterogeneous and toxic substrates beyond lignin. Curr Opin Biotechnol 73:1–13.
709 9. Johnson CW, Salvachúa D, Rorrer NA, Black BA, Vardon DR, John PCS, Cleveland NS, Dominick
710 G, Elmore JR, Grundl N. 2019. Innovative chemicals and materials from bacterial aromatic catabolic
711 pathways. Joule 3:1523-1537.
712 10. Linger JG, Vardon DR, Guarnieri MT, Karp EM, Hunsinger GB, Franden MA, Johnson CW, Chupka
713 G, Strathmann TJ, Pienkos PT, Beckham GT. 2014. Lignin valorization through integrated biological
714 funneling and chemical catalysis. Proc Natl Acad Sci U S A 111:12013–12018.
715 11. Masai E, Katayama Y, Fukuda M. 2007. Genetic and biochemical investigations on bacterial catabolic
716 pathways for lignin-derived aromatic compounds. Biosci Biotechnol Biochem 71:1–15.
717 12. Sonoki T, Takahashi K, Sugita H, Hatamura M, Azuma Y, Sato T, Suzuki S, Kamimura N, Masai E.
718 2018. Glucose-free *cis,cis*-muconic acid production via new metabolic designs corresponding to the
719 heterogeneity of lignin. ACS Sustainable Chem Eng 6:1256–1264.
720 13. Villar JC, Caperos A, García-Ochoa F. 2001. Oxidation of hardwood kraft-lignin to phenolic
721 derivatives with oxygen as oxidant. Wood Sci Technol 35:245–255.

14. Zhu Y, Liao Y, Lv W, Liu J, Song X, Chen L, Wang C, Sels BF, Ma L. 2020. Complementing vanillin and cellulose production by oxidation of lignocellulose with stirring control. ACS Sustainable Chem Eng 8:2361–2374.
15. Schutyser W, Renders T, Van den Bosch S, Koelewijn SF, Beckham GT, Sels BF. 2018. Chemicals from lignin: an interplay of lignocellulose fractionation, depolymerisation, and upgrading. Chem Soc Rev 47:852–908.
16. Abdelaziz OY, Ravi K, Mittermeier F, Meier S, Riisager A, Lidén G, Hulteberg CP. 2019. Oxidative depolymerization of kraft lignin for microbial conversion. ACS Sustainable Chem Eng 7:11640–11652.
17. Abdelaziz OY, Li K, Tunå P, Hulteberg CP. 2018. Continuous catalytic depolymerisation and conversion of industrial kraft lignin into low-molecular-weight aromatics. Biomass Convers Biorefinery 8:455–470.
18. Almqvist H, Veras H, Li K, García-Hidalgo J, Hulteberg C, Gorwa-Grauslund M, Parachin NS, Carlquist M. 2021. Muconic acid production using engineered *Pseudomonas putida* KT2440 and a guaiacol-rich fraction derived from kraft lignin. ACS Sustainable Chem Eng 9:8097–8106.
19. Ravi K, Abdelaziz OY, Nöbel M, García-Hidalgo J, Gorwa-Grauslund MF, Hulteberg CP, Lidén G. 2019. Bacterial conversion of depolymerized Kraft lignin. Biotechnol Biofuels 12:56.
20. Navas LE, Dexter G, Liu J, Levy-Booth D, Cho M, Jang SK, Mansfield SD, Renneckar S, Mohn WW, Eltis LD. 2021. Bacterial transformation of aromatic monomers in softwood black liquor. Front Microbiol 12:735000.
21. Brunel F, Davison J. 1988. Cloning and sequencing of *Pseudomonas* genes encoding vanillate demethylase. J Bacteriol 170:4924–4930.
22. Priefert H, Rabenhorst J, Steinbüchel A. 1997. Molecular characterization of genes of *Pseudomonas* sp. strain HR199 involved in bioconversion of vanillin to protocatechuate. J Bacteriol 179:2595–2607.
23. Abe T, Masai E, Miyauchi K, Katayama Y, Fukuda M. 2005. A tetrahydrofolate-dependent *O*-demethylase, LigM, is crucial for catabolism of vanillate and syringate in *Sphingomonas paucimobilis* SYK-6. J Bacteriol 187:2030–2037.
24. Masai E, Yamamoto Y, Inoue T, Takamura K, Hara H, Kasai D, Katayama Y, Fukuda M. 2007. Characterization of *ligV* essential for catabolism of vanillin by *Sphingomonas paucimobilis* SYK-6. Biosci Biotechnol Biochem 71:2487–2492.
25. Chen HP, Chow M, Liu CC, Lau A, Liu J, Eltis LD. 2012. Vanillin catabolism in *Rhodococcus jostii* RHA1. Appl Environ Microbiol 78:586–588.
26. Fleige C, Hansen G, Kroll J, Steinbüchel A. 2013. Investigation of the *Amycolatopsis* sp. strain ATCC 39116 vanillin dehydrogenase and its impact on the biotechnical production of vanillin. Appl Environ

755 Microbiol 79:81–90.
756 27. Ding W, Si M, Zhang W, Zhang Y, Chen C, Zhang L, Lu Z, Chen S, Shen X. 2015. Functional
757 characterization of a vanillin dehydrogenase in *Corynebacterium glutamicum*. Sci Rep 5:8044.
758 28. Mallinson SJB, Machovina MM, Silveira RL, Garcia-Borràs M, Gallup N, Johnson CW, Allen MD,
759 Skaf MS, Crowley MF, Neidle EL, Houk KN, Beckham GT, DuBois JL, McGeehan JE. 2018. A
760 promiscuous cytochrome P450 aromatic *O*-demethylase for lignin bioconversion. Nat Commun
761 9:2487.
762 29. García-Hidalgo J, Ravi K, Kuré LL, Lidén G, Gorwa-Grauslund M. 2019. Identification of the two-
763 component guaiacol demethylase system from *Rhodococcus rhodochrous* and expression in
764 *Pseudomonas putida* EM42 for guaiacol assimilation. AMB Express 9:34.
765 30. Barton N, Horbal L, Starck S, Kohlstedt M, Luzhetskyy A, Wittmann C. 2018. Enabling the
766 valorization of guaiacol-based lignin: Integrated chemical and biochemical production of *cis*,*cis*-
767 muconic acid using metabolically engineered *Amycolatopsis* sp ATCC 39116. Metab Eng 45:200–210.
768 31. Suzuki Y, Otsuka Y, Araki T, Kamimura N, Masai E, Nakamura M, Katayama Y. 2021. Lignin
769 valorization through efficient microbial production of β-ketoadipate from industrial black liquor.
770 Bioresour Technol 337:125489.
771 32. Tumen-Velasquez M, Johnson CW, Ahmed A, Dominick G, Fulk EM, Khanna P, Lee SA, Schmidt AL,
772 Linger JG, Eiteman MA, Beckham GT, Neidle EL. 2018. Accelerating pathway evolution by
773 increasing the gene dosage of chromosomal segments. Proc Natl Acad Sci U S A 115:7105–7110.
774 33. Qian Y, Otsuka Y, Sonoki T, Mukhopadhyay B, Nakamura M, Masai E, Katayama Y, Okamura-Abe Y,
775 Jellison J, Goodell B. 2016. Engineered microbial production of 2-pyrone-4,6-dicarboxylic acid from
776 lignin residues for use as an industrial platform chemical. Bioresources 11:6097–6109.
777 34. Shinoda E, Takahashi K, Abe N, Kamimura N, Sonoki T, Masai E. 2019. Isolation of a novel platform
778 bacterium for lignin valorization and its application in glucose-free *cis*,*cis*-muconate production. J Ind
779 Microbiol Biotechnol 46:1071–1080.
780 35. Sonoki T, Morooka M, Sakamoto K, Otsuka Y, Nakamura M, Jellison J, Goodell B. 2014.
781 Enhancement of protocatechuate decarboxylase activity for the effective production of muconate from
782 lignin-related aromatic compounds. J Biotechnol 192:71–77.
783 36. Perez JM, Kontur WS, Alherech M, Coplien J, Karlen SD, Stahl SS, Donohue TJ, Noguera DR. 2019.
784 Funneling aromatic products of chemically depolymerized lignin into 2-pyrone-4-6-dicarboxylic acid
785 with *Novosphingobium aromaticivorans*. Green Chem 21:1340–1350.
786 37. Tanihata Y, Watanabe M, Mitsukura K, Maruyama K. 2012. Oxidative degradation of 4-
787 hydroxyacetophenone in *Arthrobacter* sp. TGJ4. Biosci Biotechnol Biochem 76:838–840.

788 38. Higuchi Y, Takahashi K, Kamimura N, Masai E. 2018. Bacterial enzymes for the cleavage of lignin β-
789 aryl ether bonds: properties and applications., p 226–251. *In* Beckham GT (ed), Lignin Valorization:
790 Emerging Approaches. Royal Society of Chemistry.
791 39. Kamimura N, Takahashi K, Mori K, Araki T, Fujita M, Higuchi Y, Masai E. 2017. Bacterial catabolism
792 of lignin-derived aromatics: New findings in a recent decade: Update on bacterial lignin catabolism.
793 Environ Microbiol Rep 9:679–705.
794 40. Gall DL, Kim H, Lu F, Donohue TJ, Noguera DR, Ralph J. 2014. Stereochemical features of
795 glutathione-dependent enzymes in the *Sphingobium* sp. strain SYK-6 β-aryl etherase pathway. J Biol
796 Chem 289:8656–8667.
797 41. Tanamura K, Abe T, Kamimura N, Kasai D, Hishiyama S, Otsuka Y, Nakamura M, Kajita S, Katayama
798 Y, Fukuda M, Masai E. 2011. Characterization of the third glutathione *S*-transferase gene involved in
799 enantioselective cleavage of the β-aryl ether by *Sphingobium* sp. strain SYK-6. Biosci Biotechnol
800 Biochem 75:2404–2407.
801 42. Masai E, Ichimura A, Sato Y, Miyauchi K, Katayama Y, Fukuda M. 2003. Roles of the enantioselective
802 glutathione *S*-transferases in cleavage of β-aryl ether. J Bacteriol 185:1768–1775.
803 43. Higuchi Y, Sato D, Kamimura N, Masai E. 2020. Roles of two glutathione *S*-transferases in the final
804 step of the β-aryl ether cleavage pathway in *Sphingobium* sp. strain SYK-6. Sci Rep 10:20614.
805 44. Sato Y, Moriuchi H, Hishiyama S, Otsuka Y, Oshima K, Kasai D, Nakamura M, Ohara S, Katayama
806 Y, Fukuda M, Masai E. 2009. Identification of three alcohol dehydrogenase genes involved in the
807 stereospecific catabolism of arylglycerol-β-aryl ether by *Sphingobium* sp. strain SYK-6. Appl Environ
808 Microbiol 75:5195–5201.
809 45. Higuchi Y, Aoki S, Takenami H, Kamimura N, Takahashi K, Hishiyama S, Lancefield CS, Ojo OS,
810 Katayama Y, Westwood NJ, Masai E. 2018. Bacterial catabolism of β-hydroxypropiovanillone and β-
811 hydroxypropiosyringone produced in the reductive cleavage of arylglycerol-β-aryl ether in lignin.
812 Appl Environ Microbiol 84:e02670-17.
813 46. Niwa M, Saburi Y. 2002. Vanilloyl acetic acid as an unstable intermediate from β-
814 hydroxypropiovanillone to acetovanillone. Holzforschung 56:360–362.
815 47. Otani H, Lee YE, Casabon I, Eltis LD. 2014. Characterization of *p*-hydroxycinnamate catabolism in a
816 soil Actinobacterium. J Bacteriol 196:4293–4303.
817 48. Araki T, Tanatani K, Kamimura N, Otsuka Y, Yamaguchi M, Nakamura M, Masai E. 2020. The
818 syringate *O*-demethylase gene of *Sphingobium* sp. strain SYK-6 is regulated by DesX, while other
819 vanillate and syringate catabolism genes are regulated by DesR. Appl Environ Microbiol 86:e01712-
820 20.

821 49. Fujita M, Mori K, Hara H, Hishiyama S, Kamimura N, Masai E. 2019. A TonB-dependent receptor
822 constitutes the outer membrane transport system for a lignin-derived aromatic compound. Commun
823 Biol 2:432.
824 50. Lack A, Fuchs G. 1994. Evidence that phenol phosphorylation to phenylphosphate is the first step in
825 anaerobic phenol metabolism in a denitrifying *Pseudomonas* sp. Arch Microbiol 161:132–139.
826 51. Schmeling S, Narmandakh A, Schmitt O, Gad'on N, Schühle K, Fuchs G. 2004. Phenylphosphate
827 synthase: a new phosphotransferase catalyzing the first step in anaerobic phenol metabolism in
828 *Thauera aromatica*. J Bacteriol 186:8044–8057.
829 52. Narmandakh A, Gad'on N, Drepper F, Knapp B, Haehnel W, Fuchs G. 2006. Phosphorylation of phenol
830 by phenylphosphate synthase: role of histidine phosphate in catalysis. J Bacteriol 188:7815–7822.
831 53. Marini P, Li SJ, Gardiol D, Cronan JE, Jr., de Mendoza D. 1995. The genes encoding the biotin
832 carboxyl carrier protein and biotin carboxylase subunits of *Bacillus subtilis* acetyl coenzyme A
833 carboxylase, the first enzyme of fatty acid synthesis. J Bacteriol 177:7003–7006.
834 54. Mukhopadhyay B, Stoddard SF, Wolfe RS. 1998. Purification, regulation, and molecular and
835 biochemical characterization of pyruvate carboxylase from *Methanobacterium thermoautotrophicum*
836 strain ΔH.
837 273:5155–5166.
838 55. Wöhlbrand L, Wilkes H, Halder T, Rabus R. 2008. Anaerobic degradation of *p*-ethylphenol by
839 "*Aromatoleum aromaticum*" strain EbN1: pathway, regulation, and involved proteins. J Bacteriol
840 190:5699–5709.
841 56. Tremblay LW, Dunaway-Mariano D, Allen KN. 2006. Structure and activity analyses of *Escherichia*
842 *coli* K-12 NagD provide insight into the evolution of biochemical function in the haloalkanoic acid
843 dehalogenase superfamily. Biochemistry 45:1183–1193.
844 57. Schühle K, Fuchs G. 2004. Phenylphosphate carboxylase: a new C-C lyase involved in anaerobic
845 phenol metabolism in *Thauera aromatica*. J Bacteriol 186:4556–4567.
846 58. Schmeling S, Fuchs G. 2009. Anaerobic metabolism of phenol in proteobacteria and further studies of
847 phenylphosphate carboxylase. Arch Microbiol 191:869–878.
848 59. Lack A, Fuchs G. 1992. Carboxylation of phenylphosphate by phenol carboxylase, an enzyme system
849 of anaerobic phenol metabolism. J Bacteriol 174:3629–3636.
850 60. Takeo M, Murakami M, Niihara S, Yamamoto K, Nishimura M, Kato D, Negoro S. 2008. Mechanism
851 of 4-nitrophenol oxidation in *Rhodococcus* sp. strain PN1: characterization of the two-component 4-
852 nitrophenol hydroxylase and regulation of its expression. J Bacteriol 190:7367–7374.
853 61. Tong L. 2013. Structure and function of biotin-dependent carboxylases. Cell Mol Life Sci 70:863–891.

854 62. Biswas B, Kumar A, Krishna BB, Bhaskar T. 2021. Effects of solid base catalysts on depolymerization
855 of alkali lignin for the production of phenolic monomer compounds. Renew Energy 175:270–280.
856 63. Katahira R, Mittal A, McKinney K, Chen X, Tucker MP, Johnson DK, Beckham GT. 2016. Base-
857 catalyzed depolymerization of biorefinery lignins. ACS Sustainable Chem Eng 4:1474–1486.
858 64. Prothmann J, Sun MZ, Spégel P, Sandahl M, Turner C. 2017. Ultra-high-performance supercritical
859 fluid chromatography with quadrupole-time-of-flight mass spectrometry (UHPSFC/QTOF-MS) for
860 analysis of lignin-derived monomeric compounds in processed lignin samples. Anal Bioanal Chem
861 409:7049–7061.
862 65. Kruger JS, Cleveland NS, Zhang ST, Katahira R, Black BA, Chupka GM, Lammens T, Hamilton PG,
863 Biddy MJ, Beckham GT. 2016. Lignin depolymerization with nitrate-intercalated hydrotalcite
864 catalysts. ACS Catal 6:1316-1328.
865 66. Roberts VM, Stein V, Reiner T, Lemonidou A, Li X, Lercher JA. 2011. Towards quantitative catalytic
866 lignin depolymerization. Chem Eur J 17:5939–5948.
867 67. Beauchet R, Monteil-Rivera F, Lavoie JM. 2012. Conversion of lignin to aromatic-based chemicals
868 (L-chems) and biofuels (L-fuels). Bioresour Technol 121:328–334.
869 68. Lavoie JM, Baré W, Bilodeau M. 2011. Depolymerization of steam-treated lignin for the production
870 of green chemicals. Bioresour Technol 102:4917–4920.
871 69. Zhang T, Tremblay PL, Chaurasia AK, Smith JA, Bain TS, Lovley DR. 2013. Anaerobic benzene
872 oxidation via phenol in *Geobacter metallireducens*. Appl Environ Microbiol 79:7800–7806.
873 70. Holmes DE, Risso C, Smith JA, Lovley DR. 2012. Genome-scale analysis of anaerobic benzoate and
874 phenol metabolism in the hyperthermophilic archaeon *Ferroglobus placidus*. ISME J 6:146–157.
875 71. Du L, Ma L, Qi F, Zheng X, Jiang C, Li A, Wan X, Liu SJ, Li S. 2016. Characterization of a unique
876 pathway for 4-cresol catabolism initiated by phosphorylation in *Corynebacterium glutamicum*. J Biol
877 Chem 291:6583–6594.
878 72. Seifried A, Schultz J, Gohla A. 2013. Human HAD phosphatases: structure, mechanism, and roles in
879 health and disease. FEBS J 280:549–571.
880 73. Chapman-Smith A, Cronan Jr. JE. 1999. In vivo enzymatic protein biotinylation. Biomol Eng 16:119–
881 125.
882 74. Bower S, Perkins J, Yocum RR, Serror P, Sorokin A, Rahaim P, Howitt CL, Prasad N, Ehrlich SD,
883 Pero J. 1995. Cloning and characterization of the *Bacillus subtilis birA* gene encoding a repressor of
884 the biotin operon. J Bacteriol 177:2572–2575.
885 75. Breinig S, Schiltz E, Fuchs G. 2000. Genes involved in anaerobic metabolism of phenol in the
886 bacterium *Thauera aromatica*. J Bacteriol 182:5849–5863.

887 76. Jobst B, Schühle K, Linne U, Heider J. 2010. ATP-dependent carboxylation of acetophenone by a
888 novel type of carboxylase. J Bacteriol 192:1387–1394.
889 77. Weidenweber S, Schühle K, Demmer U, Warkentin E, Ermler U, Heider J. 2017. Structure of the
890 acetophenone carboxylase core complex: prototype of a new class of ATP-dependent
891 carboxylases/hydrolases. Sci Rep 7:39674.
892 78. Fukuhara Y, Inakazu K, Kodama N, Kamimura N, Kasai D, Katayama Y, Fukuda M, Masai E. 2010.
893 Characterization of the isophthalate degradation genes of *Comamonas* sp. strain E6. Appl Environ
894 Microbiol 76:519-527.
895 79. Johnson M, Zaretskaya I, Raytselis Y, Merezhuk Y, McGinnis S, Madden TL. 2008. NCBI BLAST: a
896 better web interface. Nucleic Acids Res 36:W5-W9.
897 80. Li W, Cowley A, Uludag M, Gur T, McWilliam H, Squizzato S, Park YM, Buso N, Lopez R. 2015.
898 The EMBL-EBI bioinformatics web and programmatic tools framework. Nucleic Acids Res 43:W580-
899 W584.
900 81. Sievers F, Wilm A, Dineen D, Gibson TJ, Karplus K, Li W, Lopez R, McWilliam H, Remmert M,
901 Söding J, Thompson JD, Higgins DG. 2011. Fast, scalable generation of high-quality protein multiple
902 sequence alignments using Clustal Omega. Mol Syst Biol 7:539.
903 82. Kaczmarczyk A, Vorholt JA, Francez-Charlot A. 2012. Markerless gene deletion system for
904 Sphingomonads. Appl Environ Microbiol 78:3774–3777.
905 83. Silva-Rocha R, Martínez-García E, Calles B, Chavarría M, Arce-Rodríguez A, de Las Heras A, Páez-
906 Espino AD, Durante-Rodríguez G, Kim J, Nikel PI, Platero R, de Lorenzo V. 2013. The Standard
907 European Vector Architecture (SEVA): a coherent platform for the analysis and deployment of
908 complex prokaryotic phenotypes. Nucleic Acids Res 41:D666-75.
909 84. Katayama Y, Nishikawa S, Nakamura M, Yano K, Yamasaki M, Morohoshi N, Haraguchi T. 1987.
910 Cloning and expression of *Pseudomonas paucimobilis* SYK-6 genes involved in the degradation of
911 vanillate and protocatechuate in *P. putida*. Mokuzai Gakkaishi 33:77–79.
912 85. Nagata Y, Kato H, Ohtsubo Y, Tsuda M. 2019. Lessons from the genomes of lindane-degrading
913 sphingomonads. Environ Microbiol Rep 11:630–644.
914 86. Studier FW, Moffatt BA. 1986. Use of bacteriophage T7 RNA polymerase to direct selective high-
915 level expression of cloned genes. J Mol Biol 189:113–130.
916 87. Bolivar F, Backman K. 1979. Plasmids of *Escherichia coli* as cloning vectors. Methods Enzymol
917 68:245–267.
918 88. Figurski DH, Helinski DR. 1979. Replication of an origin-containing derivative of plasmid RK2
919 dependent on a plasmid function provided in *trans*. Proc Natl Acad Sci U S A 76:1648–1652.

920 89. Blatny JM, Brautaset T, Winther-Larsen HC, Karunakaran P, Valla S. 1997. Improved broad-host-range
921 RK2 vectors useful for high and low regulated gene expression levels in gram-negative bacteria.
922 Plasmid 38:35–51.
923 90. Kaczmarczyk A, Vorholt JA, Francez-Charlot A. 2013. Cumate-inducible gene expression system for
924 Sphingomonads and other *Alphaproteobacteria*. Appl Environ Microbiol 79:6795–6802.
925

TABLE 1. Strains and plasmids used in this study

Strain or plasmid	Relevant characteristic(s)[a]	Reference or source
Strains		
Sphingobium sp.		
SYK-6	Wild type; NBRC 103272/JCM 17495, Nal^r Sm^r	(84)
Δ06490 (SME062)	SYK-6 derivative; ΔSLG_06490 (*acvF*), Nal^r Sm^r	This study
Δ06500 (SME063)	SYK-6 derivative; ΔSLG_06500 (*acvE*), Nal^r Sm^r	This study
Δ06510 (SME064)	SYK-6 derivative; ΔSLG_06510 (*acvD*), Nal^r Sm^r	This study
Δ06520 (SME065)	SYK-6 derivative; ΔSLG_06520 (*acvC*), Nal^r Sm^r	This study
Δ06530 (SME066)	SYK-6 derivative; ΔSLG_06530 (*acvB*), Nal^r Sm^r	This study
Δ06540 (SME067)	SYK-6 derivative; ΔSLG_06540 (*acvA*), Nal^r Sm^r	This study
Δ06550 (SME068)	SYK-6 derivative; ΔSLG_06550 (*acvR*), Nal^r Sm^r	This study
Sphingobium japonicum		
UT26S	Type strain, NBRC 101211/JCM17232, γ-hexachlorocyclohexane degradation	(85)
Pseudomonas sp.		
NGC7	Wild type	(34)
NGC703	NGC7 derivative; Δ*pcaHG catB*	(34)
Escherichia coli		
BL21(DE3)	F$^-$ *ompT hsdSB*(r_B^- m_B^-) *gal dcm* (DE3); T7 RNA polymerase gene under the control of the *lacUV5* promoter	(86)
HB101	*recA13 supE44 hsd20 ara-14 proA2 lacY1 galK2 rpsL20 xyl-5 mtl-1*	(87)
NEB 10-beta	Δ(*ara-leu*) *7697 araD139 fhuA* Δ*lacX74 galK16 galE15 e14-* ϕ*80dlacZ*Δ*M15 recA1 relA1 endA1 nupG rpsL* (Sm^r) *rph spoT1* Δ(*mrr-hsdRMS-mcrBC*)	New England Biolabs
Plasmids		
pRK2013	Tra$^+$ Mob$^+$ ColE1 replicon, Km^r	(88)
pAK405	Plasmid for allelic exchange and markerless gene deletions in sphingomonads, Km^r	(82)
pJB861	RK2 broad-host-range expression vector; P_m *xylS*, Km^r	(89)
pET-21a(+)	Expression vector; T7 promoter, Ap^r	Novagen
pET-16b	Expression vector; T7 promoter, Ap^r	Novagen
pQF	Expression vector; Q5 promoter, codon-optimized *cymR*, Tc^r	(90)
pUC118	Cloning vector; lactose promoter (P_{lac}), Ap^r	Takara Bio
pSEVA241	pRO1600/ColE1 replicon, Km^r	(83)
pTS093	pJB866 with a 0.2-kb PCR amplified fragment containing P_{lac} from pUC118	(12)
pTS032	pUC118 with a 1.6-kb KpnI fragment carrying *aroY*	(35)
pJHV01	pJB866 with a 4.6-kb BamHI PCR amplified fragment carrying *hpvZ*, SLG_20400, *vceA*, and *vceB*	(5)
pAK06490	pAK405 with a 1.7-kb deletion cassette carrying up-and downstream regions of *acvF*	This study
pAK06500	pAK405 with a 1.6-kb deletion cassette carrying up-and downstream regions of *acvE*	This study
pAK06510	pAK405 with a 1.6-kb deletion cassette carrying up-and downstream regions of *acvD*	This study
pAK06520	pAK405 with a 1.4-kb deletion cassette carrying up-and downstream regions of *acvC*	This study
pAK06530	pAK405 with a 1.6-kb deletion cassette carrying up-and downstream regions of *acvB*	This study
pAK06540	pAK405 with a 1.7-kb deletion cassette carrying up-and downstream regions of *acvA*	This study
pAK06550	pAK405 with a 1.8-kb deletion cassette carrying up-and downstream regions of *acvR*	This study
pE21*acv*	pET-21a(+) with a 7.4-kb PCR amplified fragment carrying *acvABCDEF*	This study
pJB*acv*	pJB861 with a 7.4-kb NotI fragment carrying *acvABCDEF* from pE21*acv*	This study
pE16*acvA*	pET-16b with a 1.8-kb PCR amplified fragment carrying *acvA*	This study
pE16*acvB*	pET-16b with a 1.0-kb PCR amplified fragment carrying *acvB*	This study
pE16*acvF*	pET-16b with a 0.8-kb PCR amplified fragment carrying *acvF*	This study
pE16*acvCDE*	pET-16b with a 3.4-kb PCR amplified fragment carrying *acvCDE*	This study
pQF*acvCDE*	pQF with a 3.3-kb PCR amplified fragment carrying *acvCDE*	This study
pSEVA241_P_{lac}	pSEVA241 with a 0.2-kb PCR amplified fragment containing P_{lac} from pUC118	This study
pSEVA*acv*	pSEVA241_P_{lac} with a 7.4-kb NotI fragment carrying *acvABCDEF* from pJB*acv*	This study
pQF*vce*	pQF with a 1.4-kb PCR amplified fragment carrying *vceA* and *vceB* from pJHV01	This study
pTS093*vce*	pTS093 with a 1.4-kb PCR amplified fragment carrying *vceA* and *vceB* from pQF*vce*	This study
pTS093*vce-aroY*	pTS093*vce* with a 1.6-kb KpnI fragment carrying *aroY* from pTS032	This study

[a]Nal^r, Sm^r, Km^r, Tc^r, and Ap^r, resistance to nalidixic acid, streptomycin, kanamycin, tetracycline, and ampicillin, respectively.

TABLE 2. Primers used in this study

Gene, plasmid, or strain	Primer	Sequence (5' to 3')
For RT-PCR		
Amplified region 1	570-560_F	ATAGCCATGAAAGGGATGCG
	570-560_R	AGGAGAACGAGGATTTCCGC
Amplified region 2	560-550_F	CGGCAGATATTTCTCCAGCC
	560-550_R	CCTTGATGCTACAGATCGGC
Amplified region 3	550-540_F	GTGTGCGTCGTCTCGATG
	550-540_R	TGCTGGAGACGATGGTCG
Amplified region 4	540-530_F	AGGATTGCGGTTTCCACCAT
	540-530_R	TACTGCGAGCACTGGTACAC
Amplified region 5	530-520_F	GCGTTGATTTCCACCAGTCC
	530-520_R	ATGGTGGAAACCGCAATCCT
Amplified region 6	520-510_F	CGTTTCCTCCACCAGCTTCT
	520-510_R	GGACTGGTGGAAATCAACGC
Amplified region 7	510-500_F	CGTGAAACCCGCATCGA
	510-500_R	CATGTCGAGGTGCAGGTACT
Amplified region 8	500-490_F	CTGTTCGGCGTGAAGAGATG
	500-490_R	GCCTATCTCCAGCACCAGTT
Amplified region 9	490-480_F	CAGCACGAAATCGAACGGTC
	490-480_R	CATCTCTTCACGCCGAACAG
For plasmid construction		
pAK06550	06550top_F	GCAAGCTTCCTGTGCGCCTTCATCG
	06550bottom_R	GATATTTCTCCAGCCAGCCGAATTCGCTGGAACTCCAGCTATGGTCG
pAK06550 and pAK06540	06550bottom-06540top_F	GCGAATTCGGCTGGCTGGAGAAATATC
	06550bottom-06540top_R	CGCTTTCCAGCTCATAATGGGATCCCGTGGAACTGGCAGTAATAGGG
pAK06540 and pAK06530	06540bottom-06530top_F	CGGGATCCCATTATGAGCTGGAAAGCG
	06540bottom-06530top_R	CCCTCGATGGTGATGACCTCTAGACGCGTGTCGAGATCGTTCGG
pAK06530 and pAK06520	06530bottom-06520top_F	CGTCTAGACGGTCATCACCATCGAGGG
	06530bottom-06520top_R	CACTTCGCCATGCTCCACGAATTCGCGCGTTGATTTCCACCAGTC
pAK06520 and pAK06510	06520bottom-06510top_F	GCGAATTCGTGGAGCATGGCGAAGTG
	06520bottom-06510top_R	ATTGATGCGGCATTCGATGGGTACCGCATCGTCCAGATCCTCGACC
pAK06510 and pAK06500	06510bottom-06500top_F	GCGGTACCCATCGAATGCCGCATCAAT
	06510bottom-06500top_R	GGCAACTGGTGCTGGAGATTCTAGACGTGGGGCTCAGCGTGAAGAC
pAK06500 and pAK06490	06500bottom-06490top_F	CGTCTAGAATCTCCAGCACCAGTTGCC
	06500bottom-06490top_R	GTCTCGACCTTGGGATCAGGATCCCGCTTGTAGCCGCCCAGATTG
pAK06490	06490bottom_F	CGGGATCCTGATCCCAAGGTCGAGAC
	06490bottom_R	GCGGTACCTGATGCGGGCGGAAATCTC
pE21*acv*	*acvA-acvF*_F	AAGGAGATATACAGCGGCCGCGCGCGGAAAAGAGCATATGA
	*acvA-acvF*_R	GCTCGAATTCGGATCTTATGCCAGCGGGAATGC
pE16*acvA*	pE16*acvA*_F	TCGAAGGTCGTCATATGAGCGAACCGACCAAG
	pE16*acvA*_R	GTTAGCAGCCGGATCCTCATGCGTCCTCCAGAAC
pE16*acvB*	pE16*acvB*_F	TCGAAGGTCGTCATATGACGGCCGCCGTCTCC
	pE16*acvB*_R	GTTAGCAGCCGGATCCTTATCTGCGTCCCCCGAA
For plasmid construction		
pE16*acvF*	pE16*acvF*_F	TCGAAGGTCGTCATATGACCGCCCCCTTCACC
	pE16*acvF*_R	GTTAGCAGCCGGATCCTCAGCCCAGCAGGCCGAG

pE16*acvCDE*	pE16*acvCDE*_F	TCGAAGGTCGTCATATGAGCCTCACGGCAAAG
	pE16*acvCDE*_R	GTTAGCAGCCGGATCCTCAGCCATGGCTTTCCAG
pQF*acvCDE*	pQF*acvCDE*_F	CTAGTAGAGGAAGCTATGAGCCTCACGGCAAAGGA
	pQF*acvCDE*_R	TCACTTCACCGGATCTCAGCCATGGCTTTCCAGTT
pSEVA241_P_{lac}	pSEVA241_P_{lac}_F	TCACACAGGAGGCCGAGCGCCCAATACGCAAACC
	pSEVA241_P_{lac}_R	GCGCGGCCGCGGCCTCGTAATCATGGTCATAGCTG
pQF*vce*	pQF*vce*_F	TGGTCTGTTTGTAACTAGTAGAGGAGCGATTGTAAAAAGTTAAGTAA
		CACACTAAGGAGGTATTTTTATGGCCAAGACCTTCATCAC
	pQF*vce*_R	TTTTTTTTTGCGGGTCACTTCACCGTCAGGCAGCGGAGCCGAACA
pTS093*vce*	pTS093*vce*_F	TATCCTGCAGGAATTGCGATTGTAAAAAGTTAAGTAA
	pTS093*vce*_R	CACCGTACGTCTCGATCAGGCAGCGGAGCCGAA
For colony PCR		
Δ*acvR*	dis06550_conf_F	ACGGCGATGACGATCAGCTC
	dis06550_conf_R	CGTTGATGATGCGGTGATCG

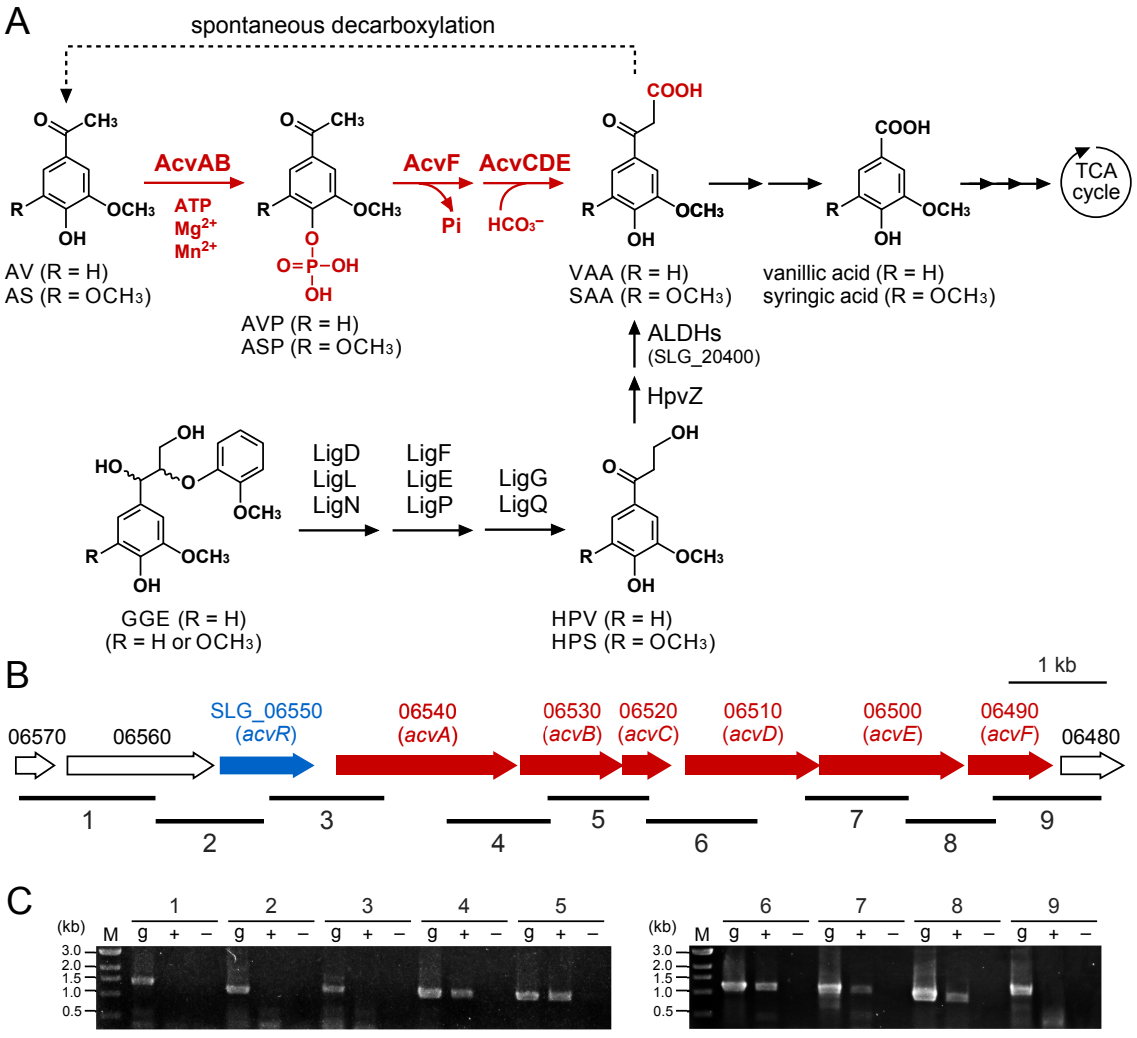

FIG 1 (A) Catabolic pathway of AV and AS in *Sphingobium* sp. strain SYK-6. The pathways for both guaiacyl (R = H)- and syringyl (R = OCH_3)-type compounds are shown. VAA, an intermediate metabolite of GGE, has been suggested to be spontaneously decarboxylated to AV (Higuchi et al., 2018; Niwa and Saburi, 2002). Enzymes: AcvAB, AVP/ASP synthetase; AcvF, AVP/ASP phosphatase; AcvCDE, biotin-dependent carboxylase; LigD, LigL, and LigN, Cα-dehydrogenases; LigF, LigE, and LigP, β-etherases; LigG and LigQ, glutathione *S*-transferases; HpvZ, HPV/HPS oxidase; ALDHs, aldehyde dehydrogenases; SLG_20400, vanilloyl acetaldehyde dehydrogenase. Abbreviations: AV, acetovanillone; AS, acetosyringone; AVP, 4-acetyl-2-methoxyphenylphosphate; ASP, 4-acetyl-2,6-dimethoxyphenylphosphate; VAA, vanilloyl acetic acid; SAA, 3-(4-hydroxy-3,5-dimethoxyphenyl)-3-oxopropanoic acid; GGE, guaiacylglycerol-β-guaiacyl ether; HPV, β-hydroxypropiovanillone; HPS, β-hydroxypropiosyringone. (B) Gene organization of *acvABCDEF*. Arrows indicate the genes from SLG_06570 to SLG_06480. (C) RT-PCR analysis of *acvABCDEF*. Total RNA used for cDNA synthesis was isolated from SYK-6 cells grown in Wx-SEMP containing 5 mM AV. The regions to be amplified are indicated by black bars below the genetic map. Lanes: M, molecular size markers; g, control PCR with the SYK-6 genomic DNA; '+' and '−', RT-PCR with and without reverse transcriptase, respectively.

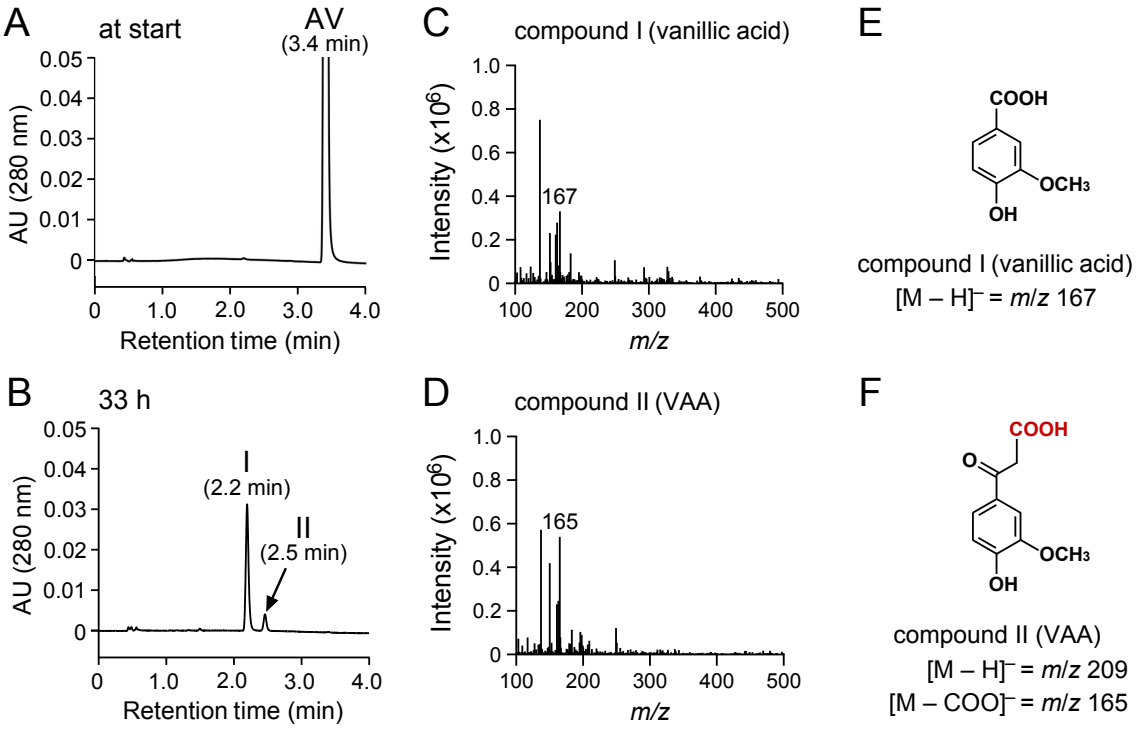

FIG 2 HPLC–MS analysis of AV metabolites. Cells of SYK-6 grown with AV (OD_{600} = 0.2) were incubated with 1 mM AV in Wx medium. Portions of the reaction mixtures were collected at the start (A) and after 33 h (B) of incubation and then analyzed by HPLC–MS. The ESI-MS spectra of compounds I and II (negative mode) are shown in panels C and D, respectively. (E and F) Chemical structures of compound I (vanillic acid) and compound II (VAA), respectively.

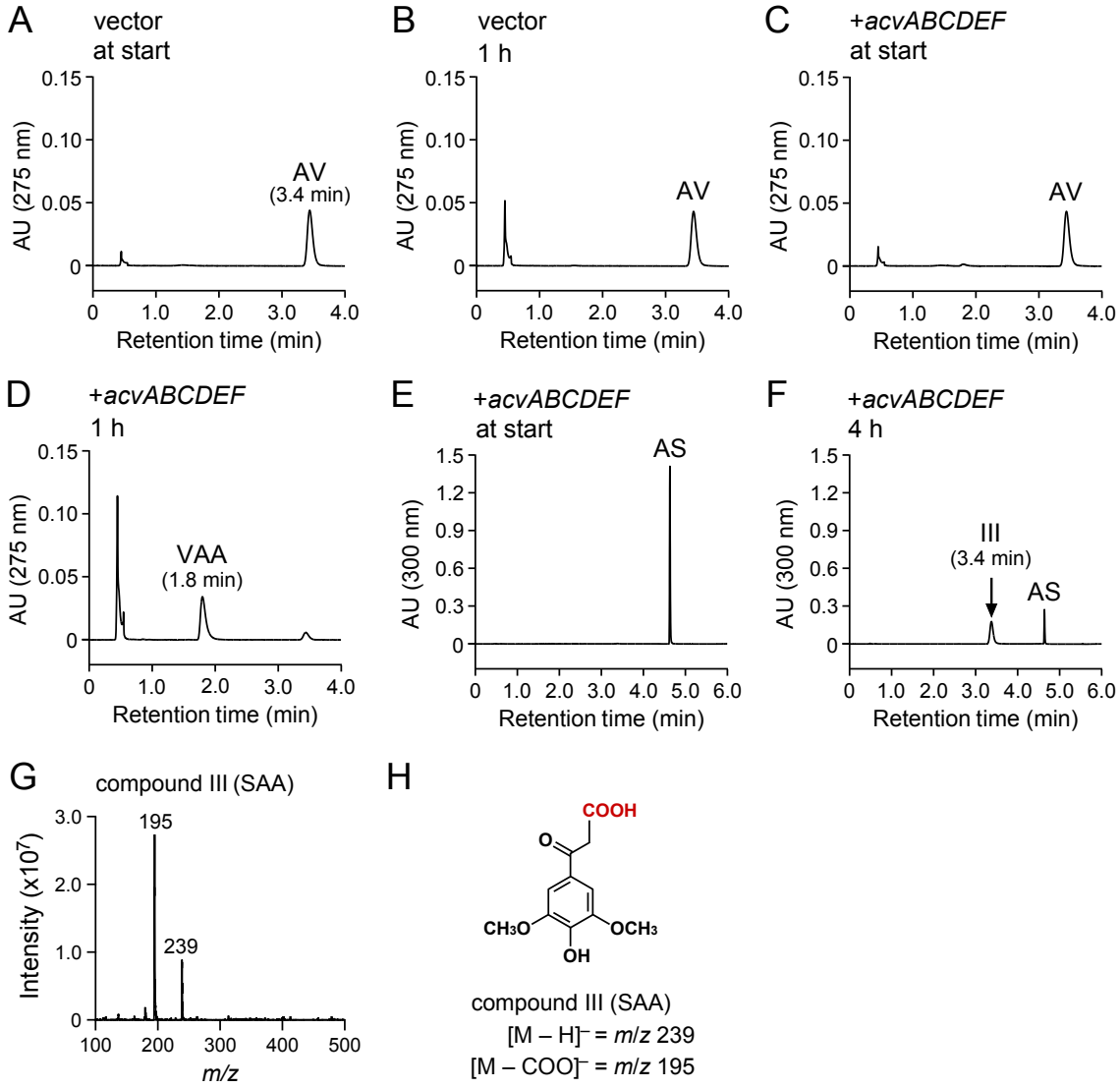

FIG 3 Conversions of AV and AS by resting cells of *S. japonicum* UT26S carrying *acvABCDEF*. Resting cells of UT26S harboring pJB861 (OD_{600} = 10.0; A and B) and resting cells of UT26S harboring pJB*acv* (OD_{600} = 10.0; C–F) were incubated with AV (200 μM; A–D) or AS (200 μM; E and F). Portions of the reaction mixtures were collected at the start (A, C, and E), after 1 h (B and D), and after 4 h (F) of incubation and analyzed by HPLC–MS. The ESI-MS spectrum of compound III (negative mode) is shown in panel G. (H) Chemical structure of compound III (SAA).

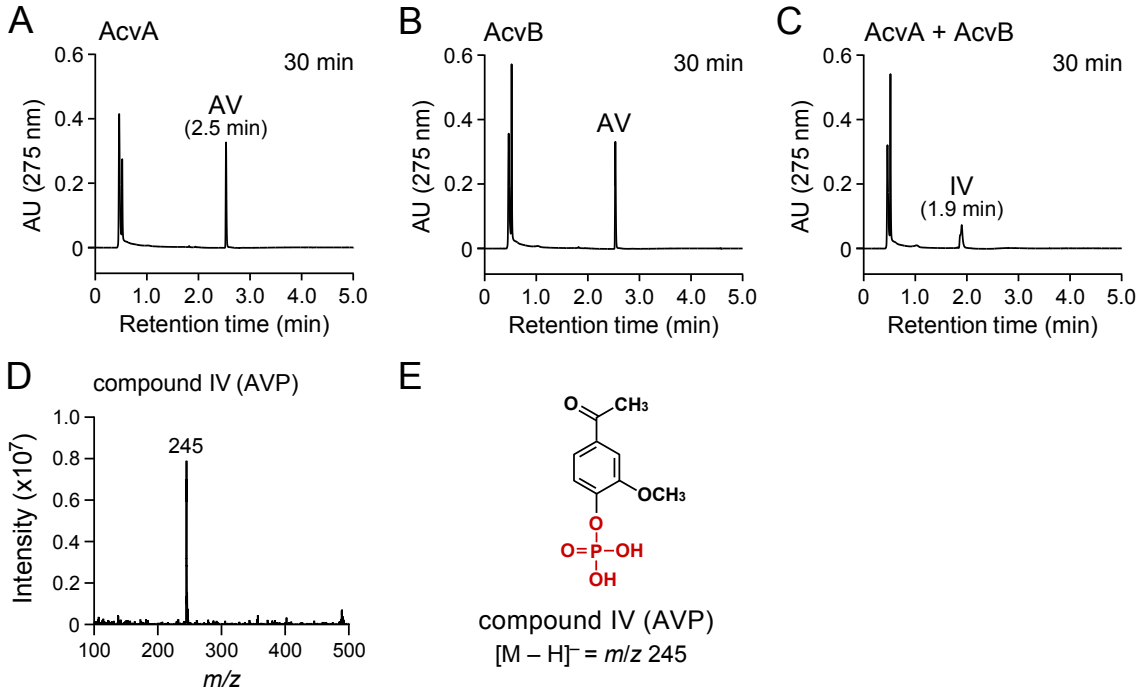

FIG 4 Conversion of AV by crude AcvA and AcvB. AV (200 µM) was incubated with a mixture of cell extracts of *E. coli* BL21(DE3) harboring pE16*acvA* and *E. coli* BL21(DE3) harboring pET-16b (500 µg protein/mL each; A), a mixture of cell extracts of *E. coli* BL21(DE3) harboring pE16*acvB* and *E. coli* BL21(DE3) harboring pET-16b (500 µg protein/mL each; B), and a mixture of cell extracts of *E. coli* BL21(DE3) harboring pE16*acvA* and *E. coli* BL21(DE3) harboring pE16*acvB* (500 µg protein/mL each; C). Reactions were performed in the presence of 2 mM ATP, 2 mM $MgCl_2$, and 200 µM $MnCl_2$. Portions of the reaction mixtures were collected after 30 min of incubation and analyzed by HPLC. The ESI-MS spectrum of compound IV (negative mode) is shown in panel D. (E) Chemical structure of compound IV (AVP).

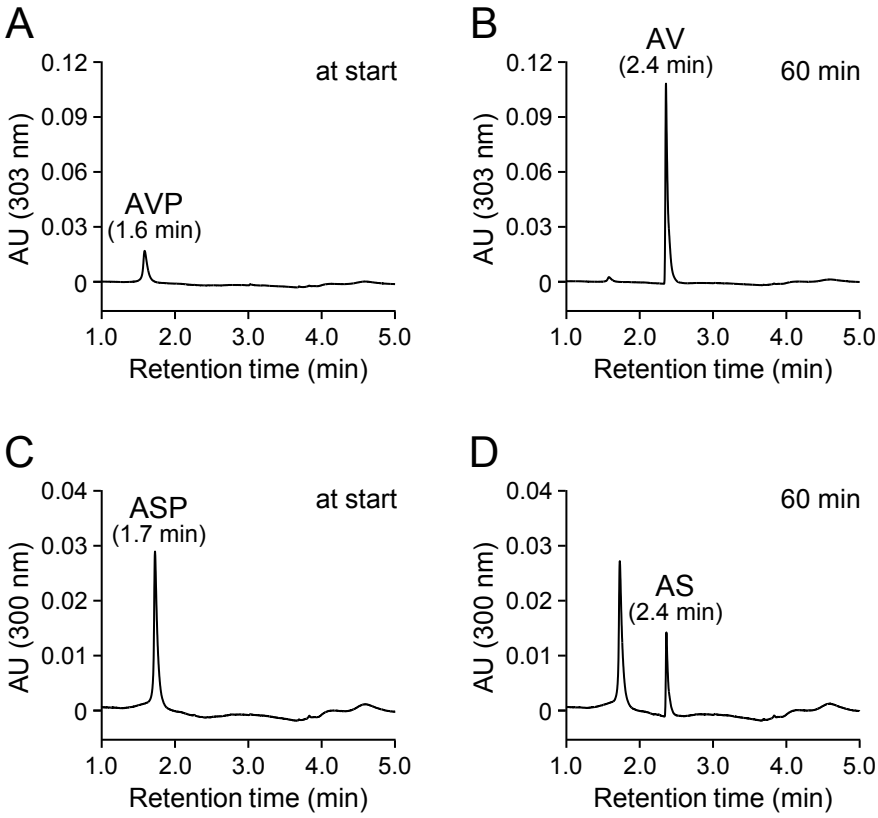

FIG 5 Conversions of AVP and ASP by AcvF. AVP (100 μM; A and B) and ASP (100 μM; C and D) were incubated with purified AcvF (5 μg protein/mL). Portions of the reaction mixtures were collected at the start (A and C) and 60 min (B and D) of incubation and analyzed by HPLC.

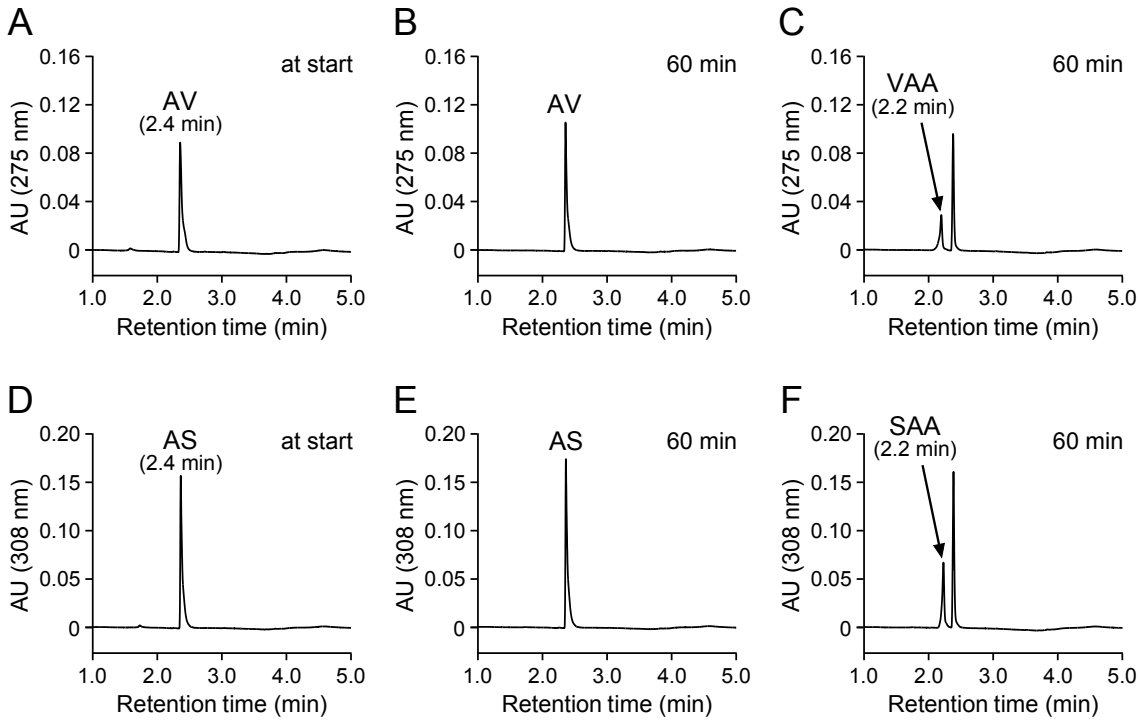

FIG 6 A mixture of AcvA-AcvB, AcvF, and AcvC-AcvD-AcvE catalyzed carboxylation of AV and AS. AV (100 μM; A–C) and AS (100 μM; D–F) were incubated with a cell extract of *S. japonicum* UT26S harboring pQF (1 mg protein/mL; A, B, D, and E) or a cell extract of UT26S harboring pQF*acvCDE* (1 mg protein/mL; C and F) in the presence of AcvA-AcvB and AcvF. Specifically, the reactions were performed in the presence of a cell extract of *E. coli* BL21(DE3) harboring pE16*acvA* (1 mg protein/mL), a cell extract of *E. coli* BL21(DE3) harboring pE16*acvB* (1 mg protein/mL), purified AcvF (10 μg protein/mL), 2 mM ATP, 2 mM $MgCl_2$, 200 μM $MnCl_2$, and 10 mM $NaHCO_3$. Portions of the reaction mixtures were collected at the start (A and D) and after 60 min (B, C, E, and F) of incubation and analyzed by HPLC.

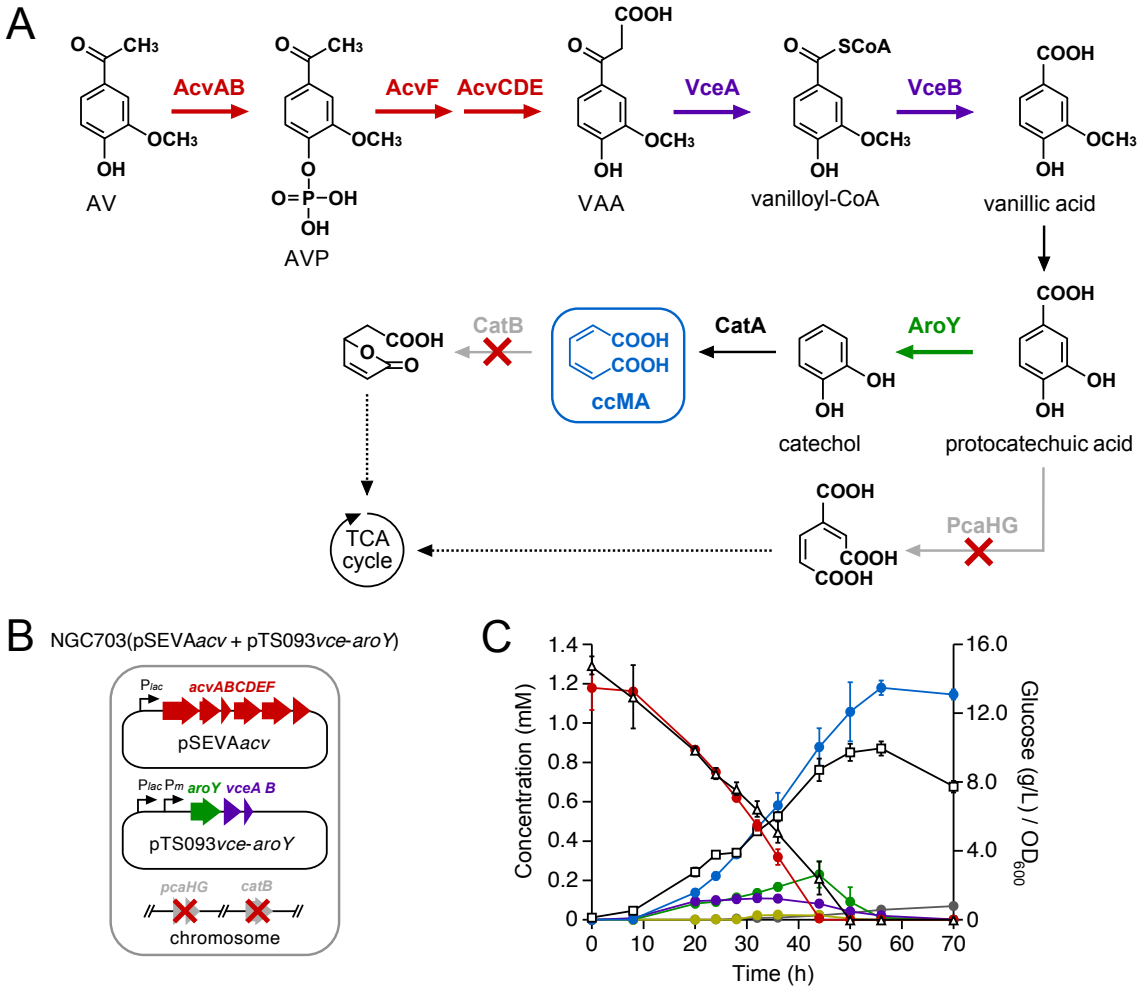

FIG 7 Production of ccMA from AV through the engineered metabolic pathway constructed in *Pseudomonas* sp. NGC7. (A) Engineered route for ccMA production from AV. Enzymes: AcvAB, AVP/ASP synthetase; AcvF, AVP/ASP phosphatase; AcvCDE, biotin-dependent carboxylase; VceA, VAA/SAA-converting enzyme; VceB, vanilloyl-CoA/syringoyl-CoA thioesterase; AroY, protocatechuic acid decarboxylase; PcaHG, protocatechuic acid 3,4-dioxygenase; CatA, catechol 1,2-dioxygenase; CatB, ccMA cycloisomerase. Abbreviations: AV, acetovanillone; AVP, 4-acetyl-2-methoxyphenylphosphate; VAA, vanilloyl acetic acid; ccMA, *cis*,*cis*-muconic acid. (B) Schematic representations of the NGC703 recombinant strain, which contains pSEVA*acv* and pTS093*vce-aroY*. (C) Conversion of 1.2 mM AV by NGC703(pSEVA*acv* + pTS093*vce-aroY*) cells during growth in MMx-3 medium containing 15 g/L glucose. The concentrations of AV (red), VAA (purple), vanillic acid (green), protocatechuic acid (mustard), ccMA (blue), and *cis*,*trans*-muconic acid (gray) were periodically measured by HPLC. The concentration of glucose (triangles) was measured by a glucose electrode. Cell growth (squares) was monitored by measuring the OD_{600}. All experiments were performed in triplicate, and each value represents the averages ± standard deviations.